Strong continentality and effective moisture drove unforeseen vegetation dynamics since the last interglacial at inland Mediterranean areas: The Villarquemado sequence in NE Iberia

P. González-Sampériz [a, *], G. Gil-Romera [a, b], E. García-Prieto [a], J. Aranbarri [c], A. Moreno [a], M. Morellón [d], M. Sevilla-Callejo [a], M. Leunda [a], L. Santos [e], F. Franco-Múgica [f], A. Andrade [g], J.S. Carrión [h], B.L. Valero-Garcés [a]

[a] *Instituto Pirenaico de Ecología, IPE—CSIC, Avda/ Montañana 1005, 50059, Zaragoza, Spain*
[b] *Department of Ecology, Faculty of Biology, Philipps-Marburg University, Marburg, Germany*
[c] *Departamento de Geografía, Prehistoria y Arqueología, Universidad del País Vasco (UPV/EHU), C/ Tomás y Valiente s/n, 01006, Vitoria-Gasteiz, Spain*
[d] *Departamento de Geodinámica, Estratigrafía y Paleontología, Facultad de Geología, Universidad Complutense de Madrid, C/ José Antonio Nováis 12, 28040, Madrid, Spain*
[e] *Facultad de Ciencias, Universidad de A Coruña, Campus da Zapateira, 15071, Coruña, Spain*
[f] *Facultad de Ecología, Universidad Autónoma de Madrid, Campus de Cantoblanco, 28049, Madrid, Spain*
[g] *Departamento de Geografía y Geología, Unidad Docente de Geología. Edificio de Ciencias, Carretera Nacional II, km. 33,600, 28871, Alcalá de Henares, Madrid, Spain*
[h] *Departamento de Biología Vegetal, Facultad de Biología, Campus de Espinardo, Universidad de Murcia, 30100, Murcia, Spain*

ARTICLE INFO

ABSTRACT

Few continental palaeoenvironmental sedimentary sequences from Southern Europe are long enough to span the last interglacial period (Marine Isotopic Stage-MIS 5), the last glacial cycle (MIS 4 to 2) and the Holocene. El Cañizar de Villarquemado (North-Eastern Iberian Peninsula) is an exceptional sedimentary lacustrine sequence spanning the last ca. 135,000 years of environmental change in an area of inland Iberia characterized by Mediterranean climate with strong continentality. We present a multiproxy study which combines palynological, sedimentological and geochemical analyses framed by an independent, robust chronology. Hydrological and climate evolutions were reconstructed by sedimentological and geochemical proxies. Development of wetlands and shallow carbonate lakes support relatively humid conditions during MIS 6, till the onset of MIS 4, and during the Holocene. Palaeohydrological conditions were drier during MIS 5 (dominance of peat environments) than during the Holocene (more frequent carbonate-producing lakes). Sedimentological evidence indicates extremely arid conditions during MIS 3 with greater activity of alluvial fans prograding into the basin. Sedimentary facies variability highlights a large environmental and hydrological variability during MIS 2 and a rapid humidity response to the onset of the Holocene.

Compared to classic Mediterranean sites, we found novel pollen assemblages for the end of MIS 6 and MIS 5 indicating that the vegetation cover was essentially represented by sustained high proportions of continentality-adapted taxa dominated by *Juniperus* during the relatively humid conditions since MIS 6 till the onset of MIS 4. Higher evapotranspiration in inland Iberia would have increased during periods of higher seasonal insolation maxima, impeding soil development and the usual mesophyte expansion during interglacials observed in other Mediterranean areas. Four main periods of forest development occurred in Villarquemado during MIS 5e, MIS 5c, MIS 5a and the Holocene; secondary peaks occurred also during MIS 3. During colder but still relatively humid MIS 4, junipers and Mediterranean taxa disappear but some mesophytes and cold-tolerant species persisted and *Pinus* became the dominant tree up to modern times. Pollen assemblages and geochemical data variability suggest a dominant control of seasonality and the impact of North Atlantic dynamics both during MIS 5 (cold events C18-C24) and full glacial conditions (HE and D-O interstadials). At millennial scales, steppe herbaceous assemblages dominated during the extremely arid conditions of MIS 3 and pines and steppe taxa during glacial period MIS 2. Villarquemado sequence demonstrates that the resilient behaviour of conifers in continental areas

---

of inland Southern European regions is key to understand the glacial–interglacial vegetation evolution and to evaluate scenarios for potential impacts of global change.

1. Introduction

The last interglacial-glacial cycle (LIG-G) including Marine Isotope Stages (MIS) 5 to 1 involves the last ~130,000 years. It is an extremely relevant time period because its ecological trends, transitions and responses may serve as potential analogue scenarios to improve projections of future climate change impacts in the environment (Cuffey and Marshall, 2000; Kukla et al., 2002; Sánchez Goñi et al., 2012; Nikolova et al., 2013). The palaeoscience research has focussed on the LIG-G transitions as these profound changes may help determining ecosystem threshold responses (e.g., Fletcher et al., 2010; Helmens, 2014). Particularly, defining the nature and rates of change at the end of the penultimate glacial stage during MIS 6 or Termination II (T-II), as well the transition between MIS 5-MIS 4 becomes critical to understand the ecosystem response to periods of rapid and intense climate change.

The palaeoclimate community is well aware that the reconstructed T-II timing may be depended on the nature of the different archives and proxies, their unique responses of climate variability, as well as uncertain chronological controls in most cases (Govin et al., 2015). The onset of Termination II ranges from 130 ka BP inferred from marine benthic $\delta^8 O$ stratigraphy (Martrat et al., 2004, 2014; Liesicki and Raymo, 2005) to 132.9 ka BP estimated with the Lago Grande di Monticchio's varve and tephra age model (Brauer et al., 2007; Wulf et al., 2012), and concurrent with the Heinrich event 11 (HE) deduced from the $\delta^{18}O$ record of Antro di Corchia stalagmite (Drysdale et al., 2009). The internal structure of T-II also shows large variability; in Monticchio for instance, the T-II entailed ca. 3 millennia of vegetation transition, with a final rapid increase of deciduous _Quercus_ and almost complete disappearance of steppe taxa announcing the rapid onset of the LIG (Allen and Huntley, 2009). In the Eastern Mediterranean sequences such as Yammouneh in Lebanon (Gasse et al., 2015), and the nearby Dead Sea (Chen and Litt, 2018), show a less abrupt, gradual transition with dominant steppe components during MIS 6 and MIS 5.

The timing of the internal phases within the LIG is also not well-resolved. MIS 5e (ca. 128-114 ka BP, Martrat et al., 2004) has been identified as one of the warmest periods of the last 800,000 years associated to higher than current sea levels (Guan et al., 2007; Sirocko et al., 2007; Rohling et al., 2008; Bardají et al., 2009; Nikolova et al., 2013). Consequently, the climate conditions of MIS 5e have been considered a relevant analogue to future warming scenarios (IPCC, 2014). Unsurprisingly, research has been focused on the previous interglacial climate behaviour compared to the current interglacial, and the possible dissimilarities caused by the Late Holocene dynamics, largely determined by unprecedented human pressure (Monastersky, 2015; Foster et al., 2017; Zalasiewicz et al., 2017; Waters et al., 2018). However, the timing of MIS 5e (and the whole MIS 5 period) in terrestrial and marine archives has also become an elusive question. Not only there are asynchronies due to archive, proxy and geographical nature (e.g., Gallup et al., 1994; Waelbroeck et al., 2002; Shackelton et al., 2003; Sirocko et al., 2007; Dabrio et al., 2011; Sier et al., 2011; Sánchez Goñi et al., 2012), but also chronological controls become challenging (Brauer et al., 2007; Govin et al., 2015).

These dissimilar patterns at a regional scale are even more striking when vegetation response to climate change is considered.

Vegetation dynamics at the LIG onset and termination greatly differs across Europe, where no single indicator can be used as a tracer of full interglacial conditions across the continent. In pollen sequences, the maximum forest expansion of the LIG has been traditionally named as "the Eemian" (Harting, 1875), but this does not always concur with the period defined as MIS 5e (Sánchez Goñi et al., 2000; Helmens et al., 2015; Camuera et al., 2019). Thus, most mid-to high-latitude sequences record an emblematic mesophyte development (deciduous oaks, birch, hazelnut and other deciduous trees) as a result of warmer and moister conditions (e.g., de Beaulieu and Reille, 1992a,b; Pons et al., 1992; Drescher-Schneider, 2000; Müller, 2000; Müller et al., 2003; Satkunas et al., 2003; Pini et al., 2009; Binka et al., 2011; Helmens et al., 2015) while Mediterranean sites record more thermophilous communities which are not always synchronous to their own mesophyte assemblages (Follieri et al., 1988; Pons and Reille, 1988; Carrión, 1992; Okuda et al., 2001; Tzedakis et al., 2002; Guiot and Cheddadi, 2004; Fernández et al., 2007; Milner et al., 2013; Camuera et al., 2019). More prominent variations are indeed registered at inner continental and/or semi-arid regions where the available sequences display large differences that prevent us from inferring generalizations (Gasse et al., 2015; Pickarski et al., 2015; Chen and Litt, 2018). Orbital parameters are often argued as the main driving force of vegetation development at glacial/interglacial time scales as summer and winter insolation fluctuations determine temperature, moisture and the interaction of both as evapotranspiration (Tzedakis, 1994; Magri and Tzedakis, 2000; Klotz et al., 2003; Braconnot et al., 2008; Camuera et al., 2019). However, as evapotranspiration is largely controlled by local factors such as latitude and altitude, it may be a main factor explaining the lack of agreement among similar plant communities across different regions.

Glacial phases (MIS 4 to MIS 2) during the LIG-G cycle do also exhibit geographical asynchronies through the Northern Hemisphere (Blunier et al., 1998; Shackleton et al., 2000; Sidall et al., 2003; Rasmussen et al., 2014) as evidenced by the different timing of maximum glacier advances at a regional scale (García-Ruiz et al., 2003; Hughes and Woodward, 2008; Lewis et al., 2009) and dissimilar climate patterns (Kageyama et al., 2013; Heiri et al., 2014; Ludwig et al., 2018). This delayed glacier advance might be related, at least in Southern Europe, to heterogeneous climate conditions during full glacial times, as suggested by varied response of vegetation formations to abrupt changes such as the Dansgaard-Oeschger cycles (D-O: Dansgaard et al., 1993; Sánchez Goñi and Harrison, 2010). Undoubtedly, discerning the vegetation evolution and its response to climate change since MIS 6 across the continent requires more Southern Europe records with a robust chronology.

In this paper we document the palynological and sedimentological sequence of El Cañizar de Villarquemado (VIL), located in a highly continental area of inner North-Eastern Iberia (Fig. 1). The VIL sequence spans the LIG-G since the MIS 6 termination to the Holocene and it is, to our knowledge, the best dated continental record of Iberia for this time interval (Valero-Garcés et al., 2019). As sedimentological and geochemical analyses on the Villarquemado sequence provide independent palaeohydrological and climate reconstructions at local and regional scale, the VIL sequence offers

an exceptional opportunity to investigate some of the critical questions on long-term terrestrial ecosystem response to climate change in the Mediterranean Basin.

Thus, the main aims of this paper are; 1) to characterize the vegetation history of VIL sequence through time and compare its response to local palaeohydrological and climate reconstructions; 2) to evaluate how orbital parameters -in particular insolation- and North Atlantic dynamics influenced the landscape evolution of inland areas of inner Iberia; and 3) to investigate analogies and different patterns among Mediterranean palynological records since the last interglacial.

2. Geographical setting

El Cañizar de Villarquemado (40°30′N, 1°18′W) is a large palaeolake of around 10−11 km^2 surface area lying at 987 m a.s.l, in the Southern Iberian Range of North-Eastern Spain (Fig. 1a). The lake basin is located within a N-S half-graben, affected by NW-SE trending normal faults (Rubio and Simón, 2007) on Mesozoic limestones. Both, Quaternary tectonics and karstic activity affected the base level of the basin, thus influencing the depositional history (Gracia et al., 2003; Gutiérrez et al., 2008, 2012). The south-central sector of this depression remained an endorheic basin until historical times, with a >3 m deep lake that was artificially drained in the 18th century (Rubio, 2004).

The climate of the region is continental Mediterranean with long cold winters and very hot summers. The maximum and minimum absolute temperatures are extreme, reaching ca. 40 °C in summer and −15 °C in winter, with strong winds and frequent below freezing temperature at night. Annual precipitation is ca. 370 mm/yr in lowlands (Cella station, 1023 m a.s.l.) reaching 740 mm/yr at higher altitudes (Griegos station, 1604 m a.s.l.). The area presents high potential evapotranspiration (>900 mm/yr, Fig. 1c). Regional-scale rainfall dynamics in Iberia is principally controlled by the westerly winds, associated with cold fronts in winter and spring and high-intensity convective storms in autumn and summer. In summer, the subtropical Azores anticyclone blocks the moisture from the west and brings warm and dry air masses from the south, increasing evapotranspiration values and the negative water balance (Fig. 1c).

The vegetation communities are dominated by *Quercus ilex* and *Q. faginea* (a semi-deciduous species), *Juniperus thurifera* and *J. phoenicea, Pinus nigra, P. pinaster* and *P. sylvestris.* Other Mediterranean shrubs abound such as *Buxus sempervirens, Juniperus sabina, Arctostaphylos uva-ursi, Erinacea anthyllis, Quercus coccifera, Rhamnus alaternus, Genista scorpius, Ephedra fragilis,* and several species of Lamiaceae, Cistaceae, and Ericaceae (Fig. 1b). The herbaceous component is composed of Poaceae (*Festuca gauthieri, Koeleria vallesiana, Stipa tenacissima*), Asteraceae (*Artemisia herba-alba, A. assoana, Santolina chamaecyparissus),* and Amaranthaceae-Chenopodiaceae *(Salsola kali, S. vermiculata).* The lowlands around the lake basin are dominated by agroforestry cultivars of
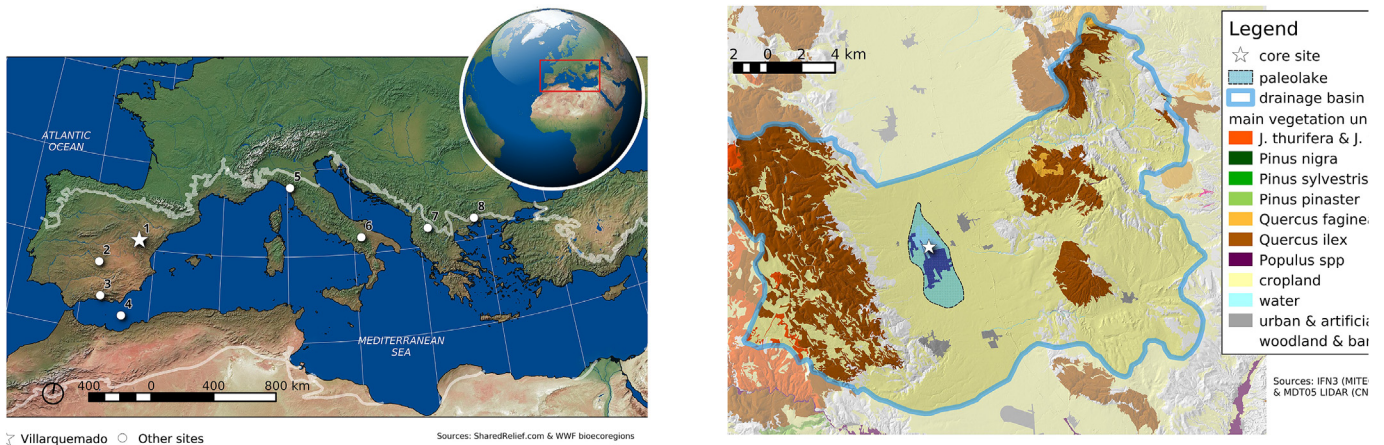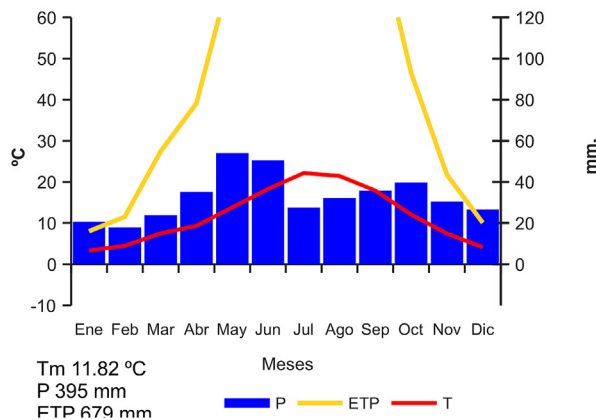

Fig. 1. A) Location of El Cañizar de Villarquemado site (white star and number 1) in NE Iberia and main palaeoenvironmental sequences considered in this discussion (white points from west to east: 2- Fuentillejo, 3- Padul, 4- ODP 977 A, 5- Corchia cave, 6- Lago Grande di Monticchio, 7- Lake Ohrid and 8- Tenaghi Philippon). B) Vegetation map of the study region. C) Climatic data for the Villarquemado area: source ACDPI (Ninyerola et al., 2005). Potential evapotranspiration calculated using Thornthwaite method (latitude).

Populus canadensis while the littoral vegetation is characterized by *Phragmites australis, Juncus acutus, J. inflexus, J. maritimus, Scirpus holoschoenus, Salix fragilis, S. atrocinerea* and *Crataegus monogyna*. The study site is therefore situated in a context of complex physiography, involving a patched vegetation, several bioclimatic belts, and the features of inland Mediterranean, continental and mountain regions.

3. Material and methods

A 74 m long sediment core was recovered from the deepest area of the palaeolacustrine basin using a truck-mounted drilling system and another 2.47 m long core was obtained with a modified 5 cm-diameter Livingstone piston corer to recover the uppermost part of the sequence. Both were stored in a 4 °C cold-room at the IPE-CSIC. Cores were correlated using sedimentary facies, radiocarbon dating and pollen stratigraphy (Aranbarri et al., 2014; Valero-Garcés et al., 2019). The composed sedimentary sequence was analysed using a multiproxy strategy, including sedimentary facies, geochemical X-Ray Fluorescence (XRF), Total Inorganic Carbon (TIC), Total Organic Carbon (TOC) and palynological analyses. Preliminary geochemical, sedimentological and pollen data were outlined in Moreno et al. (2012) and González-Sampériz et al. (2013). The Lateglacial and Holocene sequence was presented in Aranbarri et al. (2014). The new X-ray fluorescence (XRF) were obtained by the ITRAX XRF core scanner from the Large Lakes Observatory (Duluth) of the University of Minnesota (USA) using 30 s count time, 30 kV X-ray voltage, an X-ray current of 20 mA, a step size of 5 mm and a molybdenum anode X-ray tube. Some elements (Si, K, Ca, Ti, Mn, Fe, Se, Rb, Sr, Y, Zr, and Pb) and ratios were selected as indicators of carbonate productivity, sediment fluxes and redox conditions. The multiproxy strategy applied to palaeolimnological research ensures more robust environmental reconstructions, especially when strong chronological models are available (Lotter et al., 2003).

The chronology of the core was established using several techniques (mainly AMS ^{14}C for the upper 20 m and OSL and IRSL for the lower 54 m) and the age model was constructed using Bayesian techniques (Valero-Garcés et al., 2019). According to this chronological model, the Villarquemado sequence spans from 132,700 years BP (thus, the Termination II) to 246 years BP (Fig. 2).

We have analysed ca. 400 samples for fossil pollen and spores along the complete core at the IPE-CSIC palynological laboratory, with a higher resolution (one sample every 5–10 cm) at the base and the top of the sequence. Pollen extraction in samples of 5–8 gr of sediment followed the standard chemical procedure (Moore et al., 1991 modified), including treatment with HCl (37%), HF (40%), KOH (10%), mineral separation in heavy liquid (Thoulet: density 2.0 g cm-3) and incorporation of 2 tablets of *Lycopodium clavatum* exotic spores (Stockmar, 1971) to estimate pollen concentration. Palynological identification has been carried out using pollen keys (Moore et al., 1991) and photo atlases (Reille, 1992) and, specially, the reference collections from IPE-CSIC and UMU. We counted all upland and aquatic taxa. Pollen diagrams have been plotted using the package Rioja (Juggings, 2012) implemented in R and a whole of 15 pollen zones (VIL 1 to VIL 15) established following main a cluster analyses constrained by depth (CONISS) also performed with Rioja and changes from key taxa.

4. Results

4.1. The sediment sequence

Seven sedimentary units have been defined in the VIL core based on sedimentological and compositional features (Moreno et al., 2012; Valero-Garcés et al., 2019) and new XRF geochemical data (Fig. 3).

During Unit VII (74–56 m depth, ~133-100 ka BP), the sedimentary sequence is composed of an alternation of peat and carbonate layers, at decimetre to metre scale, that suggest a large variability of the depositional environments between two members: wetlands (peat deposition) and ponds (carbonate deposition). There are a number of past and recent sedimentary analogues of shallow lacustrine basins composed of a mosaic of areas with organic matter (wetlands) and carbonate accumulation (ponds) controlled by small changes in topography and hydrology (e.g., Lake Chalco, Brown et al., 2012; Lake Junin (Rodbell and Abbott, 2012). During Unit VI (56–38 m depth, ~100-71 ka BP), carbonate production decreased and clastic sediment input increased, but the basin was still likely composed of wetlands and small carbonate ponds. The onset of Unit V (38-29 m depth, ~71-59 ka BP) represents one of the largest depositional changes in the basin, with the progradation of the alluvial fans towards the centre of the basin, the development of large alluvial plains and the disappearance of the wetlands. During Unit IV (29-21 m depth, ~59-44 ka BP), distal alluvial fan and mud flat environments reached the centre of the basin. A return to previous conditions occurred during Unit III (21–15 m depth, ~44-38 ka cal BP) when lake environments developed again in the centre of the basin, surrounded by alluvial fans. During Unit II (15–3 m depth, ~38-12 ka BP) lake expanded with both clastic and carbonate facies. Finally, a carbonate lake with minor development of wetlands occurred during the deposition of Unit I (3-0 m depth, ~12-2 ka BP).

Magnetic susceptibility, elemental composition (TOC, TIC, TS) and geochemical data (XRF core scanner) values correspond well with sedimentary facies. TOC, incoherence/coherence ratio and organic matter related elements (Br) have higher values in peat facies where the organic matter is always high. Carbonate content (reflected by Ca, Sr, TIC) illustrates both clastic input of carbonates from the uplands and endogenic formation within the lake basin. Siliciclastic input (marked by Ti, Rb, Fe, Zr, and magnetic susceptibility) is higher in units II to VI and lower in those dominated by carbonate lakes and wetlands (units I and VII) (Fig. 3). Peaks of Mn mark more reducing conditions in the basin associated to peat accumulation. Raw geochemical data are included as Electronic Supplementary material (ESM).

4.2. Palynological sequence

Our average pollen sum per sample (total terrestrial pollen) was ca. 305 pollen grains (mean = 307.8, SD = 92, min = 150, max = 674). We identified ca. 180 taxa, but only a selection of them and some groups are discussed here. The raw dataset with a full list of counts and taxa, as well as plotted diagrams, can be found in Electronic Supplementary Material (ESM).

Despite near 400 pollen samples along the whole 74 m depth sequence have been analysed, only 361 of them have been considered for discussion as the remaining samples had too low pollen sums. The omitted samples held very low pollen preservation and not enough taxa diversity for statistical validity, with less than 6 different taxa preserved and thus considered as "sterile levels". These samples occur in four intervals at 93.8–87.9 ka BP, 50.1–43.1 ka BP, 35.5–31.2 ka BP and 22.3–16 ka BP (Fig. 4). According to our age model (Valero-Garcés et al., 2019), the lowermost pollen sample has an age of 131.3 ka BP and the uppermost pollen sample is 1.6 ka BP. In summary, the palynological record comprises a long sequence of ca. 130,000 years of vegetation history dominated by conifers, first *Juniperus* and then *Pinus*, the continuous but fluctuating presence of steppe taxa and woody vegetation characterized by the presence of both evergreen and semi-deciduous *Quercus* as well as Mediterranean shrubs and few
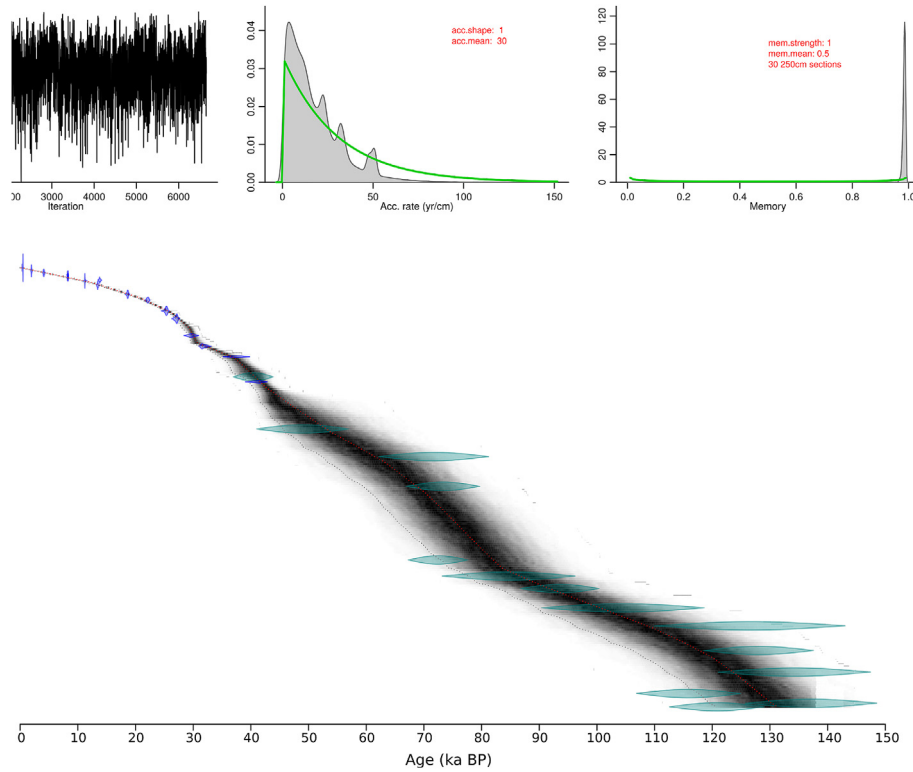
Fig. 2. Chronological Bayesian model of Villarquemado sequence based on different radiometric methods (from Valero-Garcés et al., 2019).
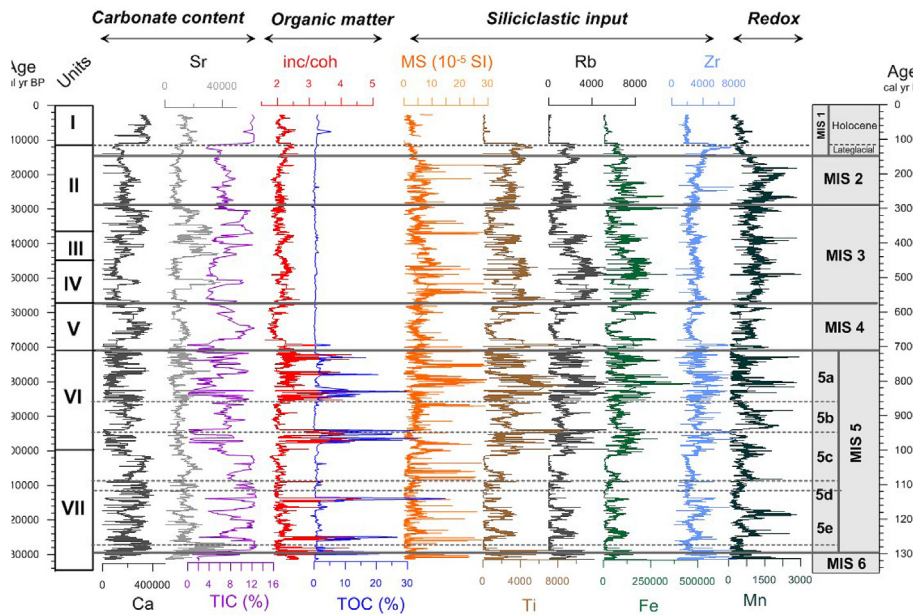

Fig. 3. Selected geochemical data of the VIL sequence plotted in age with both sedimentological units (on the left) and MIS periods (on the right) indicated. Chronological limits for MIS periods follow Lisiecki and Raymo (2005) and Rasmussen et al. (2014) while stadials and interstadials into MIS 5 chronology follow Martrat et al. (2004). All the XRF data are indicated in counts per second; inc/coh refers to the ratio among the incoherent and coherent x-ray scattering as a proxy for organic content, and MS is the magnetic susceptibility profile. Ca, Sr, and TIC are indicators of the carbonate content in the sediment while TOC and inc/coh ratio reflect the organic matter supply. Siliciclastic input is obtained from the MS values together with Ti, Rb, Fe, and Zr elements. Mn is an indicator of redox processes.

mesophytes as main components. Aquatics and local hygrophytes, including ferns, show large fluctuations owing to the hydrological variability in the basin through time.

In total, 15 pollen zones (with subzones) have been established following the main taxa changes, including ecological groupings.

The correlation between pollen zones, sedimentary units and the MIS chronological boundaries (following Martrat et al., 2004 and Rasmussen et al., 2014 chronological limits) supports the internal consistency of VIL sequence stratigraphy (Fig. 4). VIL-15 corresponds to the end of MIS 6 and the transition to MIS 5e at the
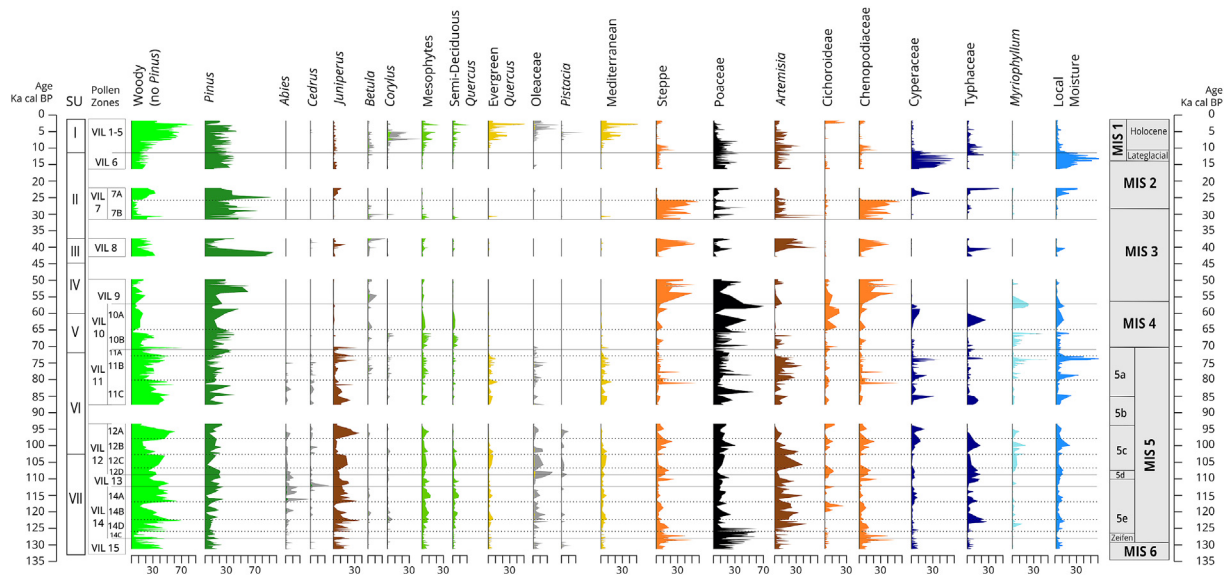
Fig. 4. Selected palynological taxa of the whole Villarquemado sequence plotted in age ka BP. Taxa included in each group (Woody, Mesophytes, Mediterranean, Steppe and Local Moisture) can be checked in ESM data (raw counts and complete diagrams). Both sedimentological and palynological zones and subzones are indicated, as well as boundaries of marine isotopic stages (MIS 6 to 1) and sub-stages including Zeifen and Lateglacial periods. White bands mark the four sterile levels regarding the pollen content. Grey shaded areas represent an exaggeration for each of the accompanying taxa: *Betula* and *Corylus* x5, Oleaceae, *Abies* and *Cedrus*, x10 and *Pistacia* x15.

bottom of the record and VIL-6 to VIL-1, on the top, to the already published Lateglacial and Holocene data (Aranbarri et al., 2014). An extended description of the whole pollen zones and subzones is included as ESM, as well as four diagrams plotting all taxa with a higher than 2% abundance. Here we only include a short summary of main trends observed.

4.2.1. Pollen zones

- VIL-15 (131.3−127 ka BP: end of MIS 6 and transition to MIS 5e). Woody taxa (without *Pinus*) record values of ca. 40%, progressively declining towards the top (Fig. 4). *Juniperus* is the main arboreal component, accompanied by mesophytes, both semideciduous and evergreen *Quercus, Abies,* Oleaceae, and *Pistacia* in lower proportions. Poaceae is important in this zone and reaches 50%. Steppe taxa fluctuate, largely increasing towards the top. *Artemisia* is noticeable, but rarely exceeds 15% while aquatics and ferns are less than 10%, showing rapid changes.
- VIL-14 to VIL-11 (127−70 ka BP: MIS 5). *Juniperus, Quercus,* and the Mediterranean taxa (mainly Oleaceae), dominate the woody component during MIS 5 (Fig. 4). Steppe taxa evolution evidences an opposite trend to that of woody communities. Besides, *Artemisia,* Cichorioideae or Amaranthaceae-Chenopodiaceae do not converge at all times. Both hygrophytes (Cyperaceae and Typhaceae) and hydrophytes such as *Myriophyllum,* reveal changing lacustrine environments. A sterile level of ca. 6 ka showed in the pollen diagram with a white band precludes any inference on vegetation dynamics between 93 and 87 ka BP (MIS 5b: Fig. 4).
- VIL-10 (71−57.5 ka BP: MIS 4). During this phase no more occurrences of Mediterranean taxa are registered where both *Quercus* types and junipers disappear. These taxa are not to be recorded again until some short episodes during MIS 3, the Lateglacial and the Holocene. Additionally, in VIL10 aquatics and hygrophytes fluctuate, indicating potentially intense environmental changes (Fig. 4).
- VIL-9, VIL-8 and sterile levels (57.5−31 ka BP: MIS 3). These zones reveal an open landscape. Steppe communities expand

and the lowest values of woody taxa are attained. Abrupt peaks of pines and hydrophytes are recorded, as well as increasing abundances of junipers and mesophytes. Synchronously, *Artemisia* rises and the remaining steppe taxa peak at the end of this period reaching one of the highest sequence abundance (Fig. 4). The local moisture group shows its lowest abundances and two periods of low pollen preservation are observed.
- VIL-7 and sterile level (31−16 ka BP: end of MIS 3 and MIS 2). Intense fluctuations of main taxa and groups characterize this period which includes the uppermost sterile level of the VIL palynological sequence (Fig. 4). The lowest mesophyte and highest steppe taxa abundances are recorded in this zone, which however show variability determined by the woody taxa, hygrophytes and local moisture proportions changes.
- VIL-6 to VIL-1 (16−1.6 ka BP: Lateglacial and Holocene, beginning of MIS 1). Aranbarri et al. (2014) recorded intense fluctuations of the dominant *Pinus* communities coexisting with few proportions of *Juniperus* and a progressive expansion of woody vegetation with maximum of *Quercus* and Mediterranean taxa at ca. 7 ka BP. *Artemisia* is still present and the hygrophytes (mainly Cyperaceae and Typhaceae) and some hydrophytes (mainly *Myriophyllum*) record abrupt changes (Fig. 4).

5. Discussion

5.1. The LIG-G period: vegetation landscape evolution and composition

Understanding how terrestrial ecosystems reacted to climate variability in continental areas during the LIG-G cannot be achieved without a comparison of well-dated, long continental records with a good geographical distribution. But we are still far from such a dataset neither globally (e.g., Anselmetti et al., 2006; Zolitschka et al., 2006; Fritz et al., 2007; Brown et al., 2012; Melles et al., 2012; Rodbell and Abbott, 2012) nor at an European scale, especially in the southern regions (e.g., Woillard, 1978; de Beaulieu and Reille, 1989; Tzedakis et al., 2003, 2006; Allen and Huntley, 2009; Litt et al., 2009; Sadori et al., 2016). In fact, large areas of the

western Mediterranean, and particularly the Iberian Peninsula, still have only a few sites with pollen data spanning as far back as MIS 6 (Carrión et al., 2013). Only Fuentillejo Maar (Vegas et al., 2010; Ortiz et al., 2013) and the new Padul (Camuera et al., 2019), and Villarquemado records, contain part of the Mid- and the Late Pleistocene time interval for inner Iberia with multiproxy analyses and independent chronological control.

5.1.1. Villarquemado sequence in the continental Iberian scenario

El Cañizar de Villarquemado record closes part of this geographical gap in Iberia (NE Spain: Fig. 1a), and it is the only available sequence that includes numerous dated intervals and not sustained by an interpolated or "tuned" chronology for the full glacial and penultimate interglacial (13 OSL and IRSL dates are located between 40 and 135 ka BP: Valero-Garcés et al., 2019). Fuentillejo and Padul (Fig. 1a) would be equivalent sequences in terms of recorded time, but the Villarquemado age model presents more robust controls, with known uncertainties for the whole sequence. In the case of Fuentillejo (68 m sequence), the age model is based on radiocarbon dates up to ca. 40 ka BP, but only linear interpolation, constrained by the identification of the Blake palaeomagnetic excursion (Galán et al., 2012) and by two U/Th dates with high errors in nahcolite samples could be carried out thereafter (Ruiz-Zapata et al., 2012). Similarly, in Padul sequence, radiocarbon dates cover the upper part of the sequence and two AAR in mollusc shells dated ca. 60 and 110 ka BP complete the age model. Age extrapolation towards the base applying a fixed sedimentation rate was proposed as the only way to provide an age control for the oldest section (Camuera et al., 2018). Thus, both dating accuracy and the uncertainty assessment of the depth-age model of VIL (Valero-Garcés et al., 2019) allow more precise discussions on the MIS 5 stadials, interstadials, the onset and duration of MIS 4, and the environmental responses to millennial scale climate fluctuations.

Previous sedimentological and compositional features (Valero-Garcés et al., 2019) and the new XRF data provide a palaeohydrological and depositional evolution of the basin and a climate reconstruction (Fig. 3). Shallow carbonate lake and wetland environments developed during the interglacials (Holocene and MIS 5), the end of MIS 6, the beginning of MIS 4 and the second half of MIS 2 (Lateglacial). Particularly during the interglacials, the alternation reflects millennial −scale variability in regional climate. A lake dominated by clastic inputs characterized glacial stages (MIS 2 and MIS 4) also showing a large depositional, climatically-induced variability. The progradation of distal alluvial fans over the basin during MIS 3 marks the most arid period of the whole recorded interval. Sedimentological and geochemical data suggest that the Eemian was wetter and warmer than the Holocene at VIL. The onset of the Holocene was rapid in terms of local palaeohydrology, as carbonate lakes developed at around 11.7 ka BP (Aranbarri et al., 2014).

The VIL sequence offers an opportunity to investigate the dynamics of the vegetation against the backdrop of climate and hydrology evolution reconstructed from sedimentological and geochemical proxies. The VIL sequence shows an open forest including Mediterranean taxa, mesophytes and conifers during the end of MIS 6 and until ca. the MIS 5 onset (127 ka BP, pollen zone VIL-15) (Fig. 5). This interval of open forested landscape at the base of the sequence is followed by a decline and another peak of woody taxa suggesting large vegetation variability during a few millennia, corresponding to the transitional period for Termination-II. The same pattern has been already identified in most Mediterranean sequences (i.e., Tzedakis, 2005; Allen and Huntley, 2009; Camuera et al., 2019). Interestingly, no Younger Dryas-like period has been identified during T-II in the Atlantic regions (Martrat et al., 2014).

Probably, Lateglacial-like climate conditions existed during this period with climate variability characterized by abrupt events as the Zeifen interstadial, dated as 130.5−127 ka BP in Iberian margin marine MD95-2042 and MD99-2331 sequences (Sánchez-Goñi et al., 2005) and also identified in VIL sequence (Fig. 5 and ESM).

The most significant feature of the VIL pollen record after the T-II termination and during the following interglacial is an increasing tree cover (higher woody percentages) since the end of MIS 6 and the occurrence of three periods of maximum development during MIS 5, broadly corresponding to MIS 5e, 5c and 5a (green bands in Fig. 6). A similar pattern with three more forested phases following summer insolation variability has also been described in main Southern European sequences located at ca. 42°N latitude as Villarquemado (Lago Grande di Monticchio, Lake Orhid or Tenaghi Philippon, from west to east: Fig. 6), as well as in some central and northern continental sites (Sánchez Goñi, 2006; Helmens, 2014). The characteristic V-shaped profiles in the VIL forest dynamics are also observed in Lake Ohrid sequence, especially for those corresponding to MIS 5c and 5a. The triple phase with the double-peaked internal structure of the vegetation forest follows closely the Alboran SST evolution during MIS 5 (Fig. 6).

Neither the three forest phases nor the "V" internal structure are recorded in other continental Iberian sequences. Fuentillejo does not include the whole MIS 5, but only the onset of MIS 5e (Ruiz-Zapata et al., 2012), preventing comparison with the other two records. Padul only shows two of the three mentioned forested intervals, during ca. MIS 5e and 5a (Camuera et al., 2019), although a short phase is also identified just at the beginning of MIS 5c. Considering that the age model is extrapolated for this interval in Padul, age uncertainties could be responsible for this apparent discrepancy (Fig. 6). The available data from the study of speleothems in the Pyrenees and Minorca caves support the view that Iberian interstadials are characterized by heterogeneous geographic patterns, both in continental and marine records, pointing to complex ocean-atmosphere teleconnections during warm intervals (Torner et al., 2019).

During the first part of MIS 4, Mediterranean sequences show a decrease of angiosperm forest trees (Fig. 6 and references related) such as observed in Area Longa, Carihuela Cave, and Abric Romaní (Gómez-Orellana et al., 2007; Fernández et al., 2007; Biltekin et al., 2019, respectively). VIL sequence also shows this continued reduction of woody vegetation after the onset of MIS 4 with minor increases during MIS 3 and MIS 2. A new noticeably forest expansion only occurs after the MIS 1 onset when all Mediterranean sequences show new forest developments (Carrión et al., 2010; González-Sampériz et al., 2010) as important, or even more, than those of MIS 5 (Fig. 6, green band on the left).

5.1.2. Unexpected vegetation communities in Villarquemado: the role of Juniperus

Regarding vegetation assemblages, the VIL vegetation sequence shows similarities with most Southern European records, but also some unique features. Particularly, during MIS 5 the occurrence and prevalence of some taxa are unexpected (Fig. 5 and ESM). Conifers but not mesophytes or Mediterranean species, are the main forest components in VIL: junipers are dominant during MIS 5 and at the end of MIS 6, while pines were paramount at the beginning of MIS 4 until the top of the sequence (Fig. 4). Surprisingly for a Mediterranean biome context, *Juniperus* fluctuations feature the woody taxa evolution during MIS 5 (Figs. 5 and 6). This might be interpreted as an inertial behaviour of juniper forests from Mid-Pleistocene onwards (Allen and Huntley, 2009; Ruiz-Zapata et al., 2012; Sadori et al., 2016; Blain et al., 2017; Gil-García et al., 2018) as it is well known that several species of *Juniperus* are adapted to water deficit and extreme temperatures (Blanco-Castro et al., 1997)
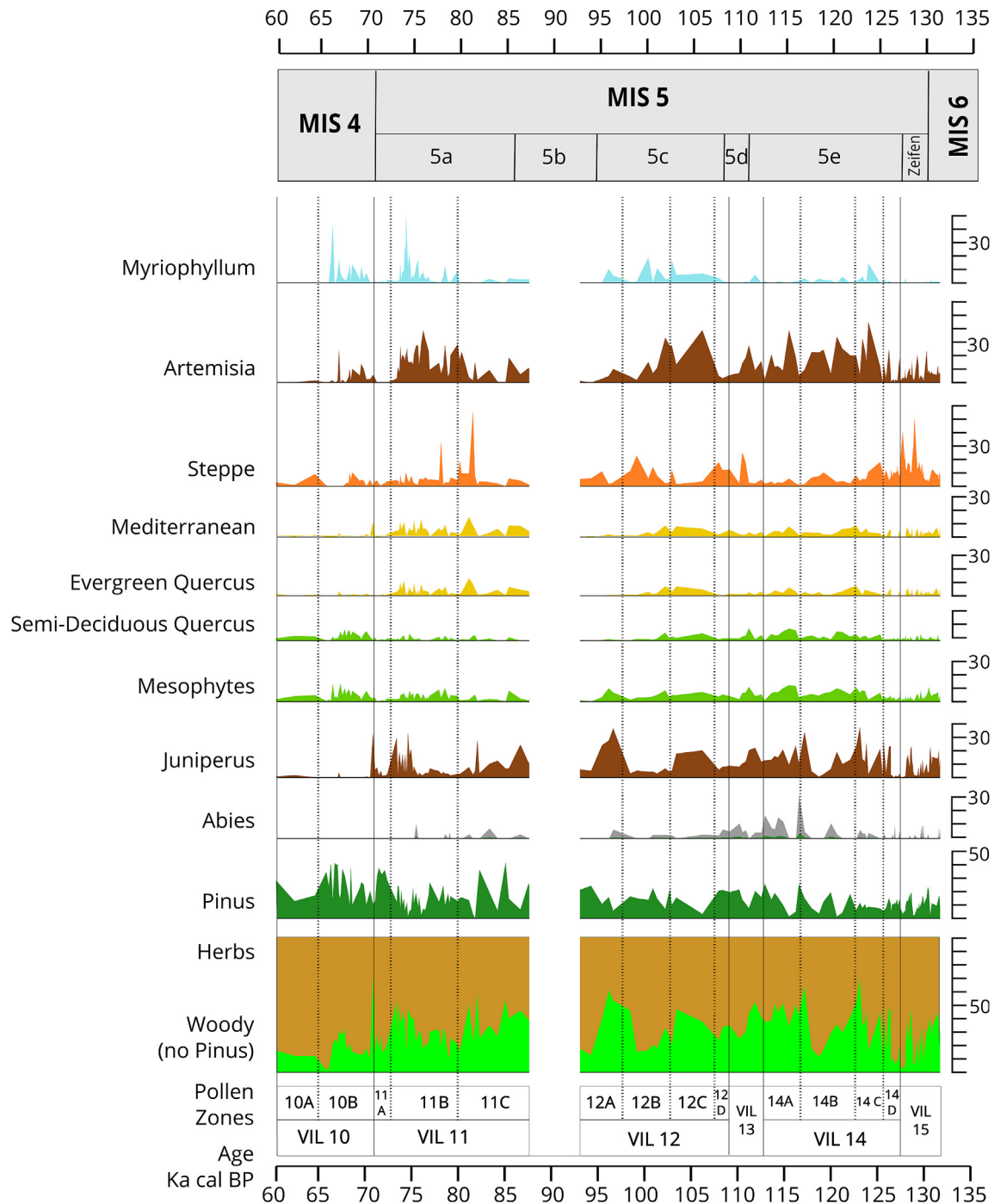
Fig. 5. Selected pollen curves (in percentages) of VIL sequence for the chronological interval 135-60 ka BP. Taxa included in each group can be checked in ESM data. Palynological zones and subzones are indicated, as well as boundaries of MIS and sub-stages including the Zeifen. Note the sterile level corresponding to MIS 5b. Grey curve of *Abies* indicates exaggeration x10.

which fits into the physiographical characteristics of the study area (Fig. 1b and c).

Juniper populations in inner Mediterranean mountains present a great adaptive capacity, high resilience levels and notable stand longevity (García et al., 1999). The Iberian *Juniperus thurifera* has been highlighted as a keystone for vegetation communities during the Pleistocene (Terrab et al., 2008) given their ability to cope with harsh, semi-arid conditions (Blanco-Castro et al., 1997) including those of full glacial periods. These populations have been suggested to be the interglacial source for recolonization (Terrab et al., 2008;

Teixeira et al., 2015). This scenario implies that the Iberian Peninsula populations, especially those at the Iberian Ranges, would have survived the MIS 6 glacial phases with an important number of individuals in the regional forests. These regions could have been likely refugia for *Juniperus* given that in the Mediterranean drought-vulnerable areas, not only temperature but especially precipitation or moisture availability are, and have been, key climate factors for vegetation development (Peñuelas et al., 2011). Evapotranspiration is indeed a critical environmental driver in western continental Mediterranean regions such as the Central
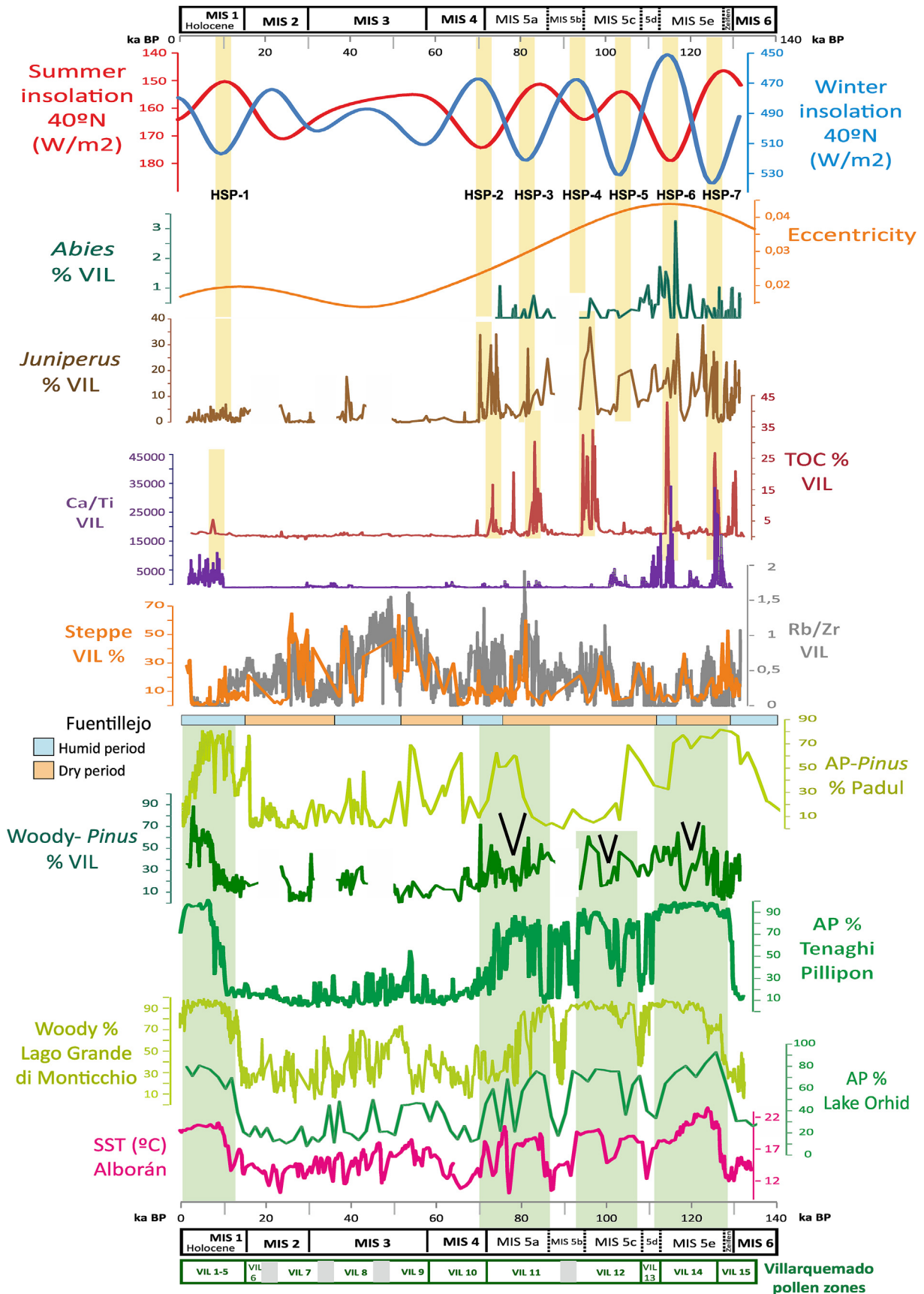
Fig. 6. From top to the bottom: a) Summer (red) and Winter (blue) insolation curves at 40° lat. N; b) HSP1 to 7 from left (Holocene) to right (boundary between MIS 5 and MIS 6) marked by yellow bands; c) Eccentricity evolution (in orange); d) *Abies* content (dark green) in VIL sequence (note that it disappears after MIS 5, just before AE-2); e) *Juniperus*

Iberian Range. These areas are not deserts but present extreme seasonal temperatures triggering an intense water deficit that distinctively determines the current vegetation composition and physiognomy (Fig. 1b and c). We argue that such intense evaporative conditions at the end of MIS 6 and most of MIS 5 would have enabled the spread and dominance of *J. thurifera*.

Interestingly, this leading role of *Juniperus* is not common in other Iberian sequences. In Padul, at the foothills of Sierra Nevada, forest assemblages during MIS 5 are dominated by pines, deciduous and evergreen *Quercus*, which is quite a general feature of Southern European pollen sequences (Camuera et al., 2019). Regarding Fuentillejo record, a more continental location similar to Villarquemado site, large *Juniperus* fluctuations occur both during MIS 6, MIS 3 and MIS 2 showing peaks associated to cold and arid conditions but unfortunately, no pollen data are available for MIS 4 and MIS 5d to 5a (Vegas et al., 2010). Molecular biomarkers suggest a succession of humid-dry periods during MIS 5 likely associated to different vegetation types (Ortiz et al., 2013) but the biomarker data do not exactly correlate with the main trends of other long Mediterranean sequences (Fig. 6). The recently published Abric Romaní palynological data spanning ca. 110-55 ka BP evidenced up to 10% of *Juniperus* during MIS 5d, but it disappears afterwards (Biltekin et al., 2019). In contrast, the anthracological data from Abric del Pastor, also placed in Eastern Iberia, reveal high frequencies of *Juniperus* along with evergreen *Quercus* and *Pistacia* during the milder phases of MIS 5 (Vidal-Matutano et al., 2015; Connolly et al., 2019). As we have mentioned before, but now regarding palynological sequences, Iberian available data show heterogeneous geographic patterns in response to complex ocean-atmosphere teleconnections and local peculiarities.

Another unique aspect of VIL record regarding vegetation dynamics is the role of *Artemisia* during MIS 6 and 5 (Fig. 4). *Artemisia* fluctuations at this time counterintuitively fit with woody taxa expansions, showing an opposite trend to Poaceae and, especially, to Amaranthaceae-Chenopodiaceae and Cichorioideae (main components of steppe taxa group besides *Ephedra*). *Artemisia* expands and contracts coevally to *Juniperus* and Mediterranean taxa pointing to similar vegetation communities than current upland steppes of inner Iberia located at 900–1200 m a.s.l. (Sainz Ollero and van Staalduinen, 2012). The surrounding alluvial fans environments in the El Cañizar de Villarquemado watershed with poor soil development could have been an optimum niche for *Artemisia* quasi-permanent communities, similarly to what occurs in current times.

Both the roles of *Juniperus* and *Artemisia* illustrate the peculiarities of vegetation dynamics in continental Iberia. Minor variations in local factors and the resilience of vegetation may produce a complex mosaic of environmental responses, which is undoubtedly a critical aspect when addressing palaeoenvironmental reconstructions and future projections of global warming impacts.

5.1.3. The three MIS 5 forested phases

The period of the maximum forest development within the last interglacial has been usually named as "Eemian" and frequently corresponds to the MIS 5e (Sánchez Goñi et al., 2005). However, in the VIL sequence, there is not a sharp boundary between the treeless and the forest-dominated landscapes, as both *Juniperus* and Mediterranean taxa peaks occurred during MIS 5e, MIS 5c and again during MIS 5a (Figs. 5 and 6, and ESM). In addition, the mentioned internal structure of forest development (V-shaped dynamics) occurred in each of the three phases. As we indicated in previous sections, the coeval evolution between woody taxa in VIL and SST in Alborán during MIS 5c and 5a, disappear during MIS 5e (Fig. 6). Thus, Eemian forests were a result of the complex interplay of ecological factors plus climatic features.

Marine sequences only identify clear interglacial conditions in Iberia after 126 ka BP (Sánchez Goñi et al., 1999, 2005). In Villarquemado, a consistent but fluctuating woody landscape in zone VIL 14C (reaching abundance values of ca. 70%) correlates with a relatively declining steppe-like vegetation (Figs. 5 and 6, and ESM). The plant landscape inferred during this forested phase reflects indeed a mosaic of different communities (steppe, savannah-like and forests) rather than a sequential succession, which is indeed one of the main long-term features of the Iberian vegetation (Carrión and Leroy et al., 2010 and papers therein).

After the mentioned decline of woody taxa at the end of MIS 5e, another conifer, *Abies*, reaches its maximum values of the whole record (VIL 14A). *Abies* maintains its presence with low percentages during MIS 5d, MIS 5c and still during MIS 5a until ca. 75 ka BP (Figs. 5 and 6). Thus, fir maximum ca. 116-113 ka BP is in good agreement with the less-seasonal climate conditions and lower summer insolation of the late Eemian (Tzedakis, 2007; Allen and Huntley, 2009). Coherently with these climatic conditions, a maximum peak of mesophytes is also recorded in VIL ca. 115 ka BP (Fig. 5).

In summary, Eemian forests in Villarquemado are unique with no clear European analogue, both in terms of composition and timing of their maximum development during the past interglacial. At that time, the landscape in the low altitude areas of the VIL basin would have been dominated by wetlands, with minor carbonate-producing ponds, while during the current interglacial, the Holocene, shallow ponds with significant carbonate production were the dominant environment in the basin. Such a landscape would indicate more humid conditions, with lesser continentality (Fig. 3), that would have created the appropriate niche for a true oak expansion during the Holocene, similarly to other Mediterranean sites dominated by oaks during interglacials (Aranbarri et al., 2014).

5.2. Orbital-scale and North Atlantic influences in Villarquemado

Considering all the orbital parameters, it is often argued that insolation during LIG-G, and particularly the timing of the summer insolation maximum, must have been the main factor controlling forest expansion (Tzedakis, 2005, 2007). In terms of vegetation dynamics, during the T-II most of the European records show the substitution of steppe herbs dominance by the expansion of forested landscapes, pointing to both precession and eccentricity as the main factors controlling insolation and therefore, vegetation development and succession (e.g., Tzedakis, 2007; Milner et al., 2013; Sadori et al., 2016). The VIL multi-proxy record might be evidencing that vegetation is broadly responding to orbital parameters similarly to other Southern European palynological

proportion's evolution (in brown) of VIL record; f) Total Organic Content −TOC percentages (in red) and g) Ca/Ti ratio (cpm) in purple of VIL sequence; h) Steppe taxa (in orange) and Rb/Zr ratio content (grey curve) following a similar evolution; i) Arid-Humid Fuentillejo periods stablished by Ortiz et al. (2013) following the relative percentage of C27%; j) Arboreal Pollen curve of Padul excluding *Pinus* (Camuera et al., 2019); k) Woody component of VIL sequence, also excluding *Pinus* ("V" structure is marked in black and forested phases by green bands; l) Tenaghi Philippon arboreal pollen-AP curve (Wijmstra, 1969; Mommersteeg et al., 1995; Tzedakis et al., 2006); m) Woody taxa evolution of Lago Grande di Monticchio sequence (Allen et al., 2000; Allen and Huntley, 2009); n) Lake Orhid arboreal pollen-AP evolution (Sadori et al., 2016); o) SST (°C) Alboran from ODP 977A (Martrat et al., 2004). MIS and boundaries of substages are included both on the top and the bottom of this figure, as well as chronological interval considered (0−140 ka BP). Pollen zones of Villarquemado sequence (with sterile levels marked in grey) are also indicated in the bottom part. (For interpretation of the references to colour in this figure legend, the reader is referred to the Web version of this article.)

sequences (Fig. 6).

5.2.1. Eccentricity and precession: the amplitude of insolation curves

Several key taxa such as *Juniperus, Abies* and those of the woody group, covariate with the eccentricity curve as it occurs in Tenaghi Philippon or Lago Grande di Monticchio (Fig. 6). Noticeably *Juniperus* in VIL reaches maximum values during periods of higher amplitude between summer and winter insolation curves, most likely driven by greater seasonality and temperature extremes. Yellow bands in Fig. 6 indicate seven "Higher Seasonality Periods" (HSP 1 to 7) in VIL record: the last and less intense during the Holocene, and the other six during MIS 5 and at the boundary with MIS 4. Coevally, maximum TOC values fit with those periods pointing to lower hydrological levels during the intervals with higher seasonality. Surely, that orbital configuration would have favoured wetland development over shallow carbonate lakes in Villarquemado basin. Additionally, the combination of less precipitation and/or intense evapotranspiration in such periods would have led to *Juniperus* thriving over other woody elements (Fig. 6).

The summer insolation maxima during MIS 5e − the most intense during the whole Pleistocene-Holocene period (Tzedakis et al., 2018) - had important implications related, not only to extreme warmth, but in the precipitation-evapotranspiration ratios in the Villarquemado area (Fig. 6). The temperature increase during the summer would have implied higher evapotranspiration and therefore increasing water deficit in soils limiting forests development, such as broadleaf communities. However, during MIS 5e and the Holocene carbonate shallow lake environments spanned (high TIC and Ca/Ti ratio) suggesting relatively moister conditions as those associated to the Eemian elsewhere (Laskar et al., 2004; Nikolova et al., 2013). These discrepancies between regional vegetation and local hydrology could also reflect the varied impact of seasonality on the different proxies (pollen *versus* geochemical data).

In sum, increased evaporation in Villarquemado area during MIS 5e -and with lower intensity during MIS 5c and MIS 5a-would be a consequence of enhanced seasonality caused by opposite summer and winter insolation during these phases. The high thermal seasonal contrast with cold winters but extremely warm summers could have prevented favourable edaphic development in these continental areas determining vegetation type's composition and the important role of *Juniperus* or *Artemisia*, as well as the better development of wetlands (peat) over shallow lakes (carbonates).

VIL geochemistry evidences that strong continentality and available effective moisture would have played a more important role in vegetation dynamics in central Iberia than temperature alone. The climate conditions during MIS 5 would have been better for forest development than those of MIS 6, and the subsequent glacial periods (MIS 4 to 2), with an overall increased moisture availability. However, water deficit would have intensified during some periods, leading to low pollen preservation levels in VIL sequence such as i.e., most part of MIS 5b (Figs. 4 and 6). At least this more arid phase had a regional reach, as the JUD-speleothem in the nearby Pyrenees (Torner et al., 2019) did not grow (hiatus) during MIS 5b.

Other examples supporting evapotranspiration as a key factor explaining vegetation variability in mid latitudes come from the Southern Levant records (Chen and Litt, 2018) where less forested landscapes predominated during the MIS 5 onset despite some mesophyte development occurred in mountain areas. The causes for low effective moisture phases during glacial and interglacial periods have to be found in both the variability of orbital configuration (increased seasonality), but also regional microclimate conditions (high altitude, continentality), enabling a strong and persistent seasonal moisture deficit, as it occurs in Villarquemado area, and facilitating the aforementioned adaptive response of *Juniperus thurifera*.

5.2.2. The North Atlantic impact in abrupt changes

In the previous sections we have shown that the VIL sequence supports the orbital control over vegetation dynamics in the Mediterranean region, but other factors such as North Atlantic circulation variability (Sánchez Goñi et al., 2005; Tzedakis et al., 2018), the particular geographical settings (Pickarski et al., 2015; Sinopoli et al., 2018; Camuera et al., 2019) and unique vegetation features of the arboreal communities of inland Iberia (Sánchez de Dios et al., 2019), may have played a critical role on plant landscape variability in areas of the Central Iberian Range affected by strong continentality.

Another plausible candidate driving vegetation fluctuations is the sequence of abrupt cold events triggered by cold water-mass expansions in the North Atlantic (Chapman and Shackleton, 1999) consistent with a reduction in the overturning circulation and resulting on decreasing inland temperatures during MIS 5e in Southern Europe (Tzedakis et al., 2018). Cold events C28 to C24 have been clearly recorded by different proxies in i.e., marine sequences MD01-2444, MD03-2664 and ODP984, as well as in Corchia Cave speleothem (Tzedakis et al., 2018) pointing to even a greater variability during the last interglacial than that observed for the present one, the Holocene. This climate instability is difficult to identify in continental sequences as land-sea correlations need to consider the age-modelling uncertainties, but in Central Iberian Range there are two records spanning this interval with enough time-resolution to capture the cold events. The C23 to C26 abrupt events have been identified in the δ^{13}C record in a speleothem from Ejulve Cave (NE Iberia), near Villarquemado, as indicative of changes in soil development and reductions in the arboreal cover (Pérez-Mejías et al., 2019). Bearing in mind age uncertainties, C24 to C28 cold events impacts may have been one of the explaining factors of *Juniperus* and Mediterranean taxa variability during that time (Fig. 7), at centennial scales.

The impact of North Atlantic abrupt changes in vegetation, in particular in *Juniperus* communities, had been previously demonstrated in the Pyrenees during glacial times (MIS 3 and MIS 2), the Lateglacial and the Early Holocene (González-Sampériz et al., 2006). In fact, the already mentioned adaptive capacity of *Juniperus* communities to continentality does not preclude sharp responses to abrupt temperature decline. Current day ecological studies show less stomatal conductance and photochemical efficiency of the photosystem of *J. thurifera* under low temperature thresholds as it presents physiological limitations under several freezing cycles (Martinez-Ferri et al., 2004; Granda et al., 2014). We suggest that probably *Juniperus* communities in Villarquemado were the dominant woody vegetation, with fluctuating values coping with cold events until ca. 70 ka BP, when abruptly disappears. Our hypothesis is that a new orbital configuration (changing eccentricity and precession) (Figs. 5 and 6) implied that cold conditions were definitively prevalent.

5.3. Full glacial conditions in continental areas: a complex scenario for great climate variability

Full glacial conditions in Europe and the North Atlantic during MIS 4 and MIS 2 included two glacial maxima, the first during MIS 4, and the second one, more severe in most European mountains, during the LGM (Hughes et al., 2013). Evidence of millennial-scale climate variability and its impact in vegetation have also been identified for this period in palynological continental sequences through Europe, with both robust chronologies and high-resolution
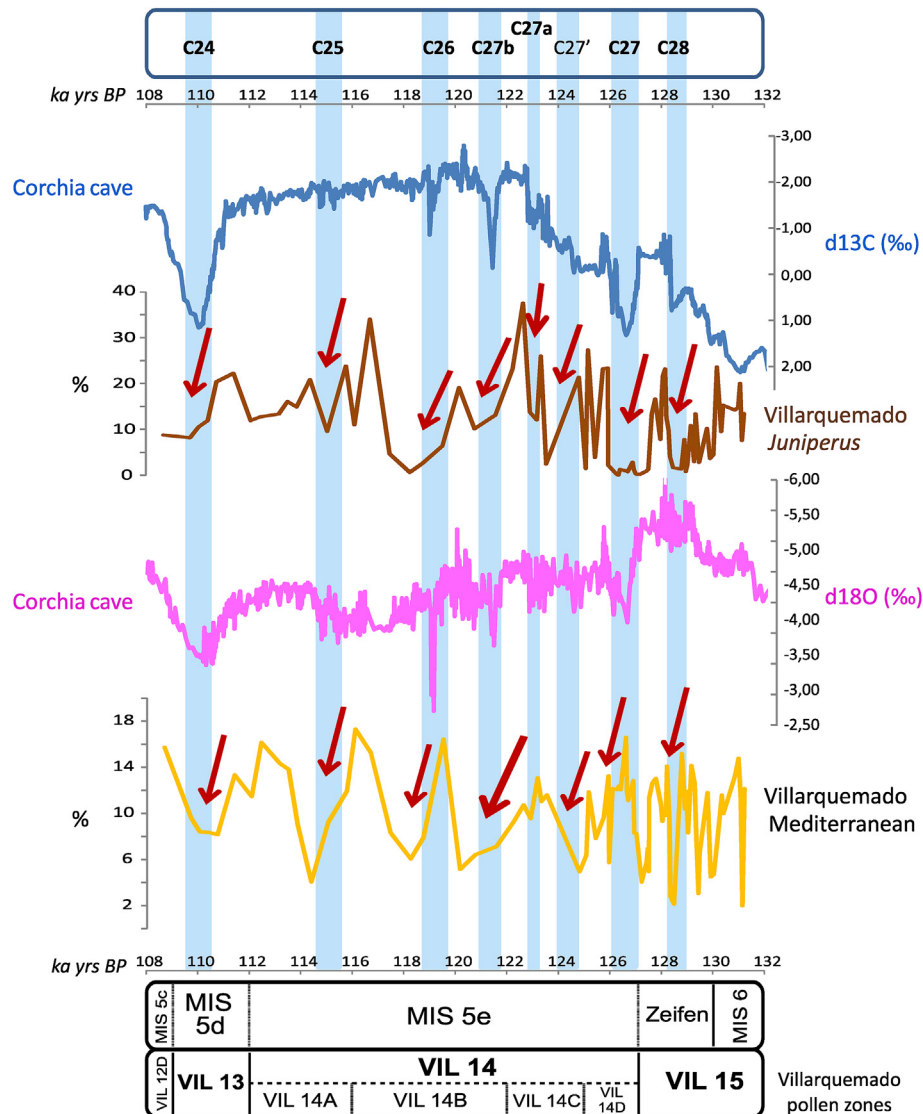
Fig. 7. Abrupt Cold events C28 to C24 (Chapman et al., 1999) identified in both stacked δ13C (in blue) and δ18O (in pink) speleothem series of Corchia Cave (Drysdale et al., 2005; Tzedakis et al., 2018), as well as in drops of *Juniperus* (in brown) and Mediterranean (in yellow) taxa content from VIL sequence. Cold events are marked by blue bands. Chronological interval considered is 132-108 ka BP. Both MIS and VIL pollen zones are also included at the bottom. (For interpretation of the references to colour in this figure legend, the reader is referred to the Web version of this article.)

pollen analyses (Allen et al., 1999; Fletcher et al., 2010; Helmens, 2014). The vegetation patterns at millennial-time scales were also modulated by orbital parameters and changes on ice volume background conditions (Tzedakis, 2005): rapid forest expansion and contraction is weaker when global ice volume is greater (MIS 4 and MIS 2) and stronger when ice volume was moderate (MIS 3). So, vegetation response to D-O events is also variable (Fletcher et al., 2010).

The interplay of orbital changes and North Atlantic dynamics results in a complex variability regarding the expansion and contraction of different key taxa during interstadials and stadials, the amplitude of changes, and the extent and composition of forests. The large geographical variability of Southern Europe, and especially of the Mediterranean region, increases the contrasting responses to abrupt climate changes (Fletcher et al., 2010 and references therein). In general, long Mediterranean sequences record a common arboreal decreasing trend from MIS 4 to MIS 2, with fluctuations and some forest recovery, especially during MIS 3 (Fig. 6). Climate variability inferred from Greenland ice cores is also

observed in VIL and other Mediterranean pollen assemblages, despite meso-thermophytes show a unique pattern. In most European sequences, thermophytes are usually absent or very scarce during stadials, but in some southern sites they have anomalous high frequencies pointing to the survival of specific tree species during the most extreme glacial phases because the location of primary refuge areas in Southern Europe and secondary ones in some inland locations as the Iberian Range (Bennet et al., 1991; Willis et al., 2000; Tzedakis et al., 2002; Médail and Diadema, 2009).

Providing a complete palaeobiogeographical model is particularly difficult in the Iberian Peninsula as continuous, high-resolution palynological records spanning the whole glacial period, with a robust and accurate chronology and multiproxy data, are scarce (see González-Sampériz et al., 2010 and references therein; Vegas et al., 2010; Biltekin et al., 2019; Camuera et al., 2019). The available sequences for the Iberian Peninsula demonstrate that steppes, parklands of conifers and refuges areas of both mesophytes and thermophytes would have coexisted in a patched

landscape during glacial times, while a clear impact of HE and D-O variability is suggested, but still not well characterized.

5.3.1. The full glacial in Villarquemado basin and the inner Iberia context

Pollen sampling in VIL sequence during MIS 4 to MIS 2 does not have the needed resolution to capture in detail vegetation abrupt changes during full glacial conditions (ESM). In addition, three intervals of low pollen preservation exits, probably as a consequence of oxidation during low lake levels and subaerial exposure conditions due to arid climate. However, the higher resolution of the geochemical data suggests, tentatively, potential impacts of HE and D-O variability in Villarquemando environmental evolution.

Sedimentological (subaerial exposure textures, distal alluvial fan depositional environments) and geochemical indicators (low values of Ca/Ti and high values Rb/Zr ratios) point to the driest conditions of the whole LIG-G cycle occurring during the second part of MIS 4 and MIS 3 time intervals. The described sedimentary facies indicate that wetlands and carbonate-producing lake environments disappear, in agreement with high Rb/Zr pointing to high siliciclastic supply to the basin and low Ca/Ti and TOC values pointing to absence of authigenic carbonates and low organic matter accumulation (Valero-Garcés et al., 2019); steppe vegetation reaches maxima and, consequently, woody taxa record their minimum values (Fig. 6 and ESM).

5.3.1.1. A relatively humid onset of MIS 4 (71-57 ka BP). The MIS 4 onset in VIL is marked by an abrupt contraction of both junipers and woody taxa that even disappear except for short events in MIS 3 (Fig. 8 and ESM). The resilient *J. thurifera* communities dominant during MIS 6 and MIS 5 were replaced by pine forest at the onset of MIS 4 and never developed significantly in the region (Fig. 4). *Pinus* progressively expanded during the glacial phase, reaching locally high abundances and the next conifer expansion occurs during the Holocene, both for *Pinus* and *Juniperus*, where junipers never reach the proportions of previous times.

Besides conifers, other persisting trees are mesophytes, mainly deciduous *Quercus* at the beginning of MIS 4 but also cold-tolerants such as *Betula* and *Alnus*, as well as Ericaceae (ESM). This is an assemblage probably promoted by cold and relatively humid conditions as suggested by geochemical data, characterizing the beginning of the full glacial (Fig. 8). Steppe herbaceous elements dominated between 60 and 40 ka BP but with a variable composition: Asteraceae are the main taxa during MIS 4 while *Ephedra* and Amaranthaceae-Chenopodiaceae, together with *Artemisia* dominate during MIS 3 (Figs. 4 and 8, and ESM). Similarly, Cyperaceae and *Juncus* expand during MIS 4 (as well as in MIS 5, MIS 2 and MIS 1: Fig. 4 and ESM) but almost disappear during MIS 3 (Fig. 8 and ESM). This community combination would be responding to the increasing aridity towards MIS 3 as indicated by Rb/Zr fluctuations, a ratio that represents the progradation of the alluvial fans and the clayish-silty material entering the basin, with lower values in MIS 4 and higher during MIS 3 (Fig. 8).

Atlantic continental records such as Area Longa in NW Iberia show high percentages of *Erica*, *Calluna* and Poaceae as well as low proportions of conifers, *Artemisia* and Amaranthaceae-Chenopodiaceae and the persistence of deciduous *Quercus*, *Corylus*, *Fagus*, *Carpinus*, *Ulmus* and *Ilex* (Gómez-Orellana et al., 2007) at the beginning of MIS 4. In the new Padul sequence, the earliest part of MIS 4 is also characterized by the abundance of Ericaceae in agreement with still humid conditions too (Camuera et al., 2019). These pollen assemblages agree with Fletcher and Sánchez Goñi (2008) who pointed out that the expansion of Ericaceae is related to minimum boreal summer insolation, and therefore, declined summer aridity and increased availability in annual moisture. In

Abric Romaní, in Northeast Spain, Burjachs et al. (2012) had identified a decrease of thermophilous taxa during MIS 4 associated to a cold and humid phase. In a recent revision Biltekin et al. (2019) however, suggest that the permanence of deciduous *Quercus* and other cold-tolerant trees like *Alnus*, *Abies*, *Betula* or *Corylus* is an evidence of nearby glacial refuge areas. The Fuentillejo sequence also shows relatively humid conditions with important oscillations for the first part of MIS 4 (until ca. 66 ka BP) in the lacustrine algae and land plants inputs (Ortiz et al., 2013).

The fluctuations in pollen records are in agreement with the chronology of the maximum advance of glaciers established in the Pyrenees for ca. 60−67 ka BP, which imply a more humid MIS 4 and then drier MIS 3 (Fig. 8). Colder climate during the early MIS 4 was not yet associated to increased aridity allowing the last maximum advance of glaciers in Mediterranean mountains (Lewis et al., 2009; Sancho et al., 2018).

5.3.1.2. The arid MIS 3 (57-29 ka BP). The MIS 3 period in VIL was the most arid phase of the whole record indicated by the progradation of alluvial fans over the lake basin as inferred from the sedimentological facies (Valero-Garcés et al., 2019). Consequently steppe vegetation dominated by Amaranthaceae-Chenopodiaceae expanded in the desiccated basin (Figs. 4 and 8, ESM). The secondary role of Asteraceae in the steppe community also supports a scenario characterized by higher aridity than previous time intervals, as usually Cichorioideae are associated to cold but not so arid climates (González-Sampériz et al., 2010). In addition, during MIS 3 pine shows large and abrupt fluctuations, deciduous *Quercus* and *Alnus* values drop and key local moisture taxa such as Cyperaceae or *Juncus* almost disappear (Figs. 4 and 8, and ESM). Two intervals of low pollen preservation occurred during this period, probably as a consequence of oxidation during sub-aerial exposure because intensification of arid conditions. Interestingly, the first sterile interval occurred after Heinrich event-HE 5 and the second one after HE 4 (Fig. 8). Maximum values of Rb/Zr ratio are also coherent with the interpretation of most arid conditions of the whole record (Figs. 6 and 8).

Padul sequence is also in agreement with dry conditions for MIS 3 although is mostly characterized by changes in temperature-related taxa (Camuera et al., 2019). Fuentillejo shows intense and prolonged dry conditions evidenced by sedimentological data (presence of dolomite-bearing facies) and, consequently, coherent pollen content (20−40% of steppe taxa and less than 10% of mesophytes) (Vegas et al., 2010). Other Iberian sequences with sedimentology or isotopes records also show arid conditions and lower water levels during MIS 3, while palynological series show increase of steppe vegetation (e.g., in Banyoles Lake: Pérez-Obiol and Julià, 1994; Höbig et al., 2012; Lacey et al., 2016; El Portalet: González-Sampériz et al., 2006; Enol lake: Moreno et al., 2010; Tagus loess records: Wolf et al., 2018).

Despite the arid conditions and the open vegetation landscape recorded in VIL, the occurrence of some peaks of woody taxa could be tentatively related with the impact of millennial-scale climate variability (Fig. 6). The interstadials of D-O 14 in pollen zone VIL-9 or D-O 8 (ca. 40 ka cal BP) in pollen zone VIL-8 marked by developments of *Juniperus*, mesophytes and Mediterranean taxa (Figs. 4 and 8) would be good examples of such impact. Similarly, maximum values of Rb/Zr ratios chronologically correspond to HE4 (39−40 ka BP), HE5 (46−47 ka BP) and HE5a (55−56 ka BP) indicating the most arid intervals, in agreement with the nearby isotope record from Ejulve Cave (Pérez-Mejías et al., 2019). The vegetation expansion occurred in MIS 4 could also potentially correlate with the impact of the interstadial phase of D-O 18 (Fig. 8). Although our proxy resolution and the uncertainty of the age model preclude definitive ascriptions of D-O or HE events during last
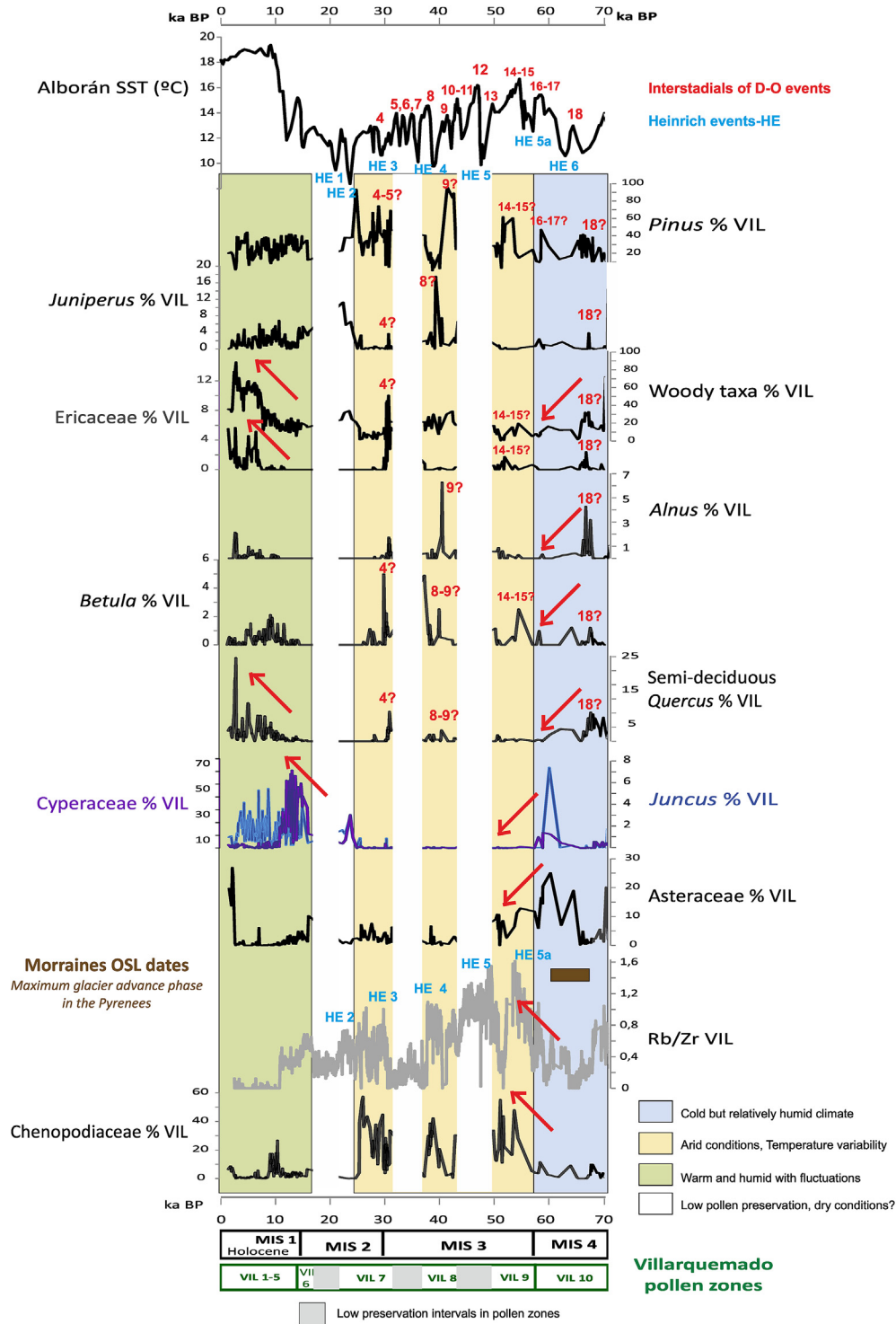
Fig. 8. Comparison of different curves from VIL sequence and regional records for 0–70 ka BP. From top to bottom: a) SST evolution (°C) in Alboran Sea from ODP 977A (Martrat et al., 2004) with both HE and D-O interstadials marked in blue and red, respectively; Selected palynological taxa percentages of VIL sequence: b) *Pinus*; c) *Juniperus*; d) Woody component; e) Ericaceae; f) *Alnus*; g) *Betula*; h) Semi-deciduous *Quercus*; i) Cyperaceae (in purple) and *Juncus* (in blue); j) Asteraceae; k) Chronological interval of Maximum Glacier advance phase stablished for the Pyrenees using OSL dates from moraines (Lewis et al., 2009; Sancho et al., 2018); l) Rb/Zr ratio of VIL record (note the highest values coevally to HE); m) Amaranthaceae-Chenopodiaceae content of VIL palynological sequence. MIS and pollen zones of Villarquemado (with sterile levels marked in grey) are included in the bottom part of the figure. Inferred climate conditions, as well as palynological sterile levels are also indicated with different colour bands: Cold but relatively humid conditions during MIS 4 is marked in blue; Aridity increase and Temperature variability is indicated for MIS 3 and the beginning of MIS 2 in yellow; Warm and humid fluctuations are associated in green for the Lateglacial and Holocene. White bands mark the sterile levels through the figure. (For interpretation of the references to colour in this figure legend, the reader is referred to the Web version of this article.)

glacial period (Fig. 8, question marks), these vegetation fluctuations are, at least, suggestive of millennial-scale variability impacts. .

In Area Longa and other pollen records from NW Iberia, three phases of deciduous woodland expansion along with smaller-scale fluctuations during MIS 3 are identified as a vegetation response to HE and D-O cycles (Muñoz-Sobrino et al., 2004; Gómez-Orellana et al., 2007; García-Moreiras et al., 2019). In most sequences (Enol, Portalet, Banyoles), some geochemical and pollen fluctuations have been interpreted not as D-O, but as HE impacts during both MIS 3 and MIS 2 (González-Sampériz et al., 2006; Moreno et al., 2010; Höbig et al., 2012; Lacey et al., 2016).

Thus, available Iberian records point to MIS 3 as the driest period of the last glacial cycle, with a patched and mosaic vegetation landscape dominated by steppe formations and generally more arid environments. Millennial-scale variability is suggested in some records, but due to the large geographical variability, new long sequences are necessary to characterize the impact of D-O and Heinrich events during MIS 3 in inner Iberia.

5.3.1.3. A variable MIS 2 (29-14 ka BP). MIS 2, the last period of the glacial phase, is characterized in VIL by greater local and regional environmental and moisture variability, as indicated by the diversity of sedimentary facies and aquatic vegetation development. Sedimentary facies indicate an increase in humidity compared to the MIS 3 interval, with the development of shallow lakes in the distal areas of the basin (Valero-Garcés et al., 2019) marked by the increase in carbonates and lower Rb/Zr ratios (Fig. 8) in contrast with drier conditions evidenced by the progradation of alluvial fans during previous stage, MIS3. At a regional scale, resilient taxa dominate with the prevalence of pines, steppe herbs, and shrubs (Figs. 4 and 8, and ESM). However, another interval of low pollen preservation (the youngest one) occurred in Villarquemado during MIS 2 (Fig. 4). This episode, although not as intense as those during MIS 3, could be the result of the occurrence of aridity spells during full glacial conditions. As we have indicated before, the LGM does not correspond with the maximum advance of glaciers in Iberia, probably because Southern Europe was influenced by more arid conditions than Central and Northern Europe at that time (Morellón et al., 2009; Fletcher et al., 2010; González-Sampériz et al., 2010; Moreno et al., 2012; Stoll et al., 2013).

Fuentillejo also shows relatively high variability during MIS 2, but is characterized by high Ti content and Magnetic susceptibility values, low TOC, reduced vegetation development and soil formation. All these indicators point to significant terrigenous inputs, abrupt periods of low lake level and major erosive processes associated to colder and more arid phases in Central Iberia since 26 ka BP (Vegas et al., 2010). Contrarily to the relatively arid conditions suggested by VIL and Fuentillejo sequences for inner Iberia during MIS 2, the Padul sequence shows that the LGM was the most extreme glacial climate of the Late Pleistocene in Southern Iberia but it was not particularly arid. This is shown by i.e., clayey carbonate facies linked to deep water environments under colder glacial conditions. As a consequence, low arboreal pollen proportions and the occurrence of *Pediastrum* is recorded, only during MIS 6 and MIS 2 in the case of *Pediastrum* (Camuera et al., 2019).

Most European and Mediterranean sequences show the lowest values of woody taxa during MIS 2 (Fletcher et al., 2010; Helmens et al., 2014) while the Iberian sequences show a more diverse vegetation dynamics. They include parkland formations, with dominant steppe vegetation and some meso-thermophytes surviving in refuge areas (Carrión et al., 2010 and references therein, González-Sampériz et al., 2010), and high proportions of conifers too, especially pines. These vegetation assemblages had a clear continuity during the beginning of the Holocene in most Mediterranean and continental areas of Iberia (Morellón et al., 2018) including Villarquemado (Aranbarri et al., 2014). Thus, the role of conifers (first *Juniperus* and then *Pinus*) in savannah-like open environments has been undoubtedly essential for both Pleistocene and Holocene vegetation history of inner Iberia (Rubiales et al., 2010). Only after the Middle Holocene and before human impact begin to shape regional vegetation, generally moister conditions and the reduced thermal amplitude allowed the spread of mixed forest (dominated in VIL by both semi-deciduous and evergreen *Quercus* as main woodland components: Figs. 4 and 8) at the same time that shallow carbonate lake developed in the centre of the basin (Aranbarri et al., 2014; Valero-Garcés et al., 2019).

This scenario is coherent with most interglacial forest expansions and moisture conditions reconstructed for the Holocene at around the Mediterranean region and Southern Europe (Roberts, 1998). However, the Villarquemado sequence (Fig. 6) indicates that MIS 1 environmental conditions have been less warm and more humid than those of MIS 5 interglacial. As we have mentioned through this work, sedimentological and geochemical results of VIL record suggests drier conditions in previous interglacial compared to the current with the dominance of wetlands and not a shallow carbonate lake. In agreement with this scenario, *Juniperus, and* not *Quercus,* has been the main tree of the dominant forest communities.

6. Conclusions

The multiproxy analysis of El Cañizar de Villarquemado sequence (NE Iberia) provides a detailed vegetation, palaeohydrological and palaeoenvironmental evolution for the last 135,000 years. Comparison of paleohydrological and paleoclimate reconstructions based on sedimentological and geochemical data with pollen data allowed an investigation of how orbital, regional and local factors have controlled the complex landscape evolution of the western Mediterranean region. Villarquemado sequence is a new multiproxy palaeoenvironmental record spanning the whole LIG-G cycle in inner areas of Southern Europe with strong continentality where few sequences are available. This new record in inner Iberia, supported by a robust chronology, illustrates the similarities of Southern European vegetation history during the LIG-G cycle, but also the uniqueness of Mediterranean regions with a high continentality.

Thus, regarding the three main aims of this work, summarized conclusions are:

(1) Vegetation history of VIL sequence through time
- Unexpected, eventual prevalence of resilient *Juniperus* communities dominates the vegetation landscape since the end of MIS 6 and during the whole MIS 5, disappearing in MIS 4. Then, *Pinus* takes the leading role during the full glacial and the Holocene. The record demonstrates the resilience of conifers in Iberian vegetation landscapes through time.
- Tree cover, represented by woody taxa expansions, records four periods of maximum development during the last 135 ka BP: the last one in the Holocene and the other three, during MIS 5e, 5c and 5a. A continued reduction of woody vegetation occurs since the first part of MIS 4 followed by minor peaks during MIS 3 and MIS 2.
- The MIS 5 forest evolution show an internal double peak "V" structure similar to that shown by some — but not all - marine and lacustrine sequences from Western and Central-Eastern Mediterranean pointing to Southern Europe heterogeneous geographic patterns during both interglacials and interstadials.

- A relatively humid onset of MIS 4 is recorded with persisting mesophytes and cold-tolerant taxa while MIS 3 showed the driest conditions of the whole LIG-G cycle with dominant steppe vegetation and fine distal alluvial fans prograding over the basin. A variable MIS 2 is characterized by the diversity of aquatic vegetation development despite resilience continue as main characteristic of regional vegetation.

(2) Orbital parameters -insolation- and North Atlantic dynamics
  - The high thermal seasonal amplitude during several phases of the last interglacial as response to orbital parameters was conducive to intense evapotranspiration triggering higher water deficit in soils. Seven Higher Seasonality Periods" (HSP1 to 7) have been recorded during the last 130 ka BP showing a close relationship with the amplitude of both summer and winter insolation curves.
  - Vegetation dynamics are usually controlled by orbital parameters, however, the North Atlantic variability at a millennial-scale (especially cold events C28 to C24 during MIS 5) also impacted in inland Iberia. The record of Heinrich events and D-O variability during full glacial times is suggested both by sedimentological proxies and some vegetation changes.
  - Local factors such as strong continentality which derive in high seasonality and evapotranspiration emerge as essential drivers too for Mediterranean vegetation dynamics.

(3) Analogies and different patterns among Mediterranean palynological records
  - Eemian forests in inner Iberia are unique with no clear European analogue. Both vegetation composition (juniper's dominance) and the dominance of wetlands point to a more continental, less humid period during the last interglacial than the Holocene due to more evapotranspiration.
  - Minor variations in local factors and the landscape resilience may produce a complex mosaic of environmental responses rather than a sequential succession in inland Mediterranean areas, which is a critical aspect when addressing future projections of global warming impacts.

Declaration of competing interest

Acknowledgements

Appendix A. Supplementary data

Supplementary data to this article can be found online at https://doi.org/10.1016/j.quascirev.2020.106425.

References

Allen, J.R.M., Huntley, B., 2009. Last Interglacial palaeovegetation, palaeoenvironments and chronology: a new record from Lago Grande di Monticchio, southern Italy. Quat. Sci. Rev. 28, 1521–1538.

Allen, J.R.M., Brandt, U., Brauer, A., Hubberten, H.W., Huntley, B., Keller, J., 1999. Rapid environmental changes in southern Europe during the last glacial period. Nature 400 (6746), 740–743.

Anselmetti, F.S., Ariztegui, D., Hodell, D.A., Hillesheim, M.B., Brenner, M., Gilli, A., McKenzie, J.A., Mueller, A.D., 2006. Late Quaternary climate-induced lake level variations in Lake Peté Itzá, Guatemala, inferred from seismic stratigraphic analysis. Palaeogeogr. Palaeoclimatol. Palaeoecol. 230, 52–69.

Aranbarri, J., González-Sampériz, P., Valero-Garcés, B., Moreno, A., Gil-Romera, G., Sevilla-Callejo, M., García-Prieto, E., Di Rita, F., Mata, M.P., Morellón, M., Magri, D., Rodríguez-Lázaro, J., Carrión, J.S., 2014. Rapid climatic changes and resilient vegetation during the Lateglacial and Holocene in a continental region of south-western Europe. Global Planet. Change 114, 50–65.

Bardají, T., Goy, J.L., Zazo, C., Hillaire-Marcel, C., Dabrio, C.J., Cabero, A., Ghaleb, B., Silva, P.G., Lario, J., 2009. Sea level and climate changes during OIS 5e in the Western Mediterranean. Geomorphology 104, 22–37.

Bennett, K.D., Tzedakis, P.C., Willis, K.J., 1991. Quaternary refugia of north European trees. J. Biogeogr. 18, 103–115.

Biltekin, D., Burjachs, F., Vallverdú, J., Sharp, W.D., Mertz-Kraus, R., Chacon, M.G., Saladie, P., Bischoff, J.L., Carbonell, E., 2019. Vegetation and climate record from abric Romaní (Capellades, northeast Iberia) during the upper Pleistocene (MIS 5d-3). Quat. Sci. Rev. 220, 154–164.

Binka, K., Nitychoruk, J., Dzierzek, J., 2011. Climate stability during the Eemian-new pollen evidence from the Nidzica site, northern Poland. Boreas 40 (2), 342–350.

Blain, H.A., Ruiz Zapata, M.B., Gil García, M.J., Sesé, C., Santonja, M., Pérez González, A., 2017. New palaeoenvironmental and palaeoclimatic reconstructions for the Middle Palaeolithic site of Cuesta de la Bajada (Teruel, eastern Spain) inferred from the amphibian and squamate reptile assemblages. Quat. Sci. Rev. 173, 78–91.

Blanco-Castro, E., Casado, M., Costa, M., Escribano, R., García-Antón, M., Génova, M., Gómez, A., Moreno, J., Morla, C., Regato, P., Sainz Ollero, H., 1997. Los Bosques Ibéricos. Una interpretación geobotánica, Barcelona. Planeta 572.

Blunier, T., Chappellaz, J., Schwander, J., Dällenbach, A., Stauffer, B., Stocker, T.F., Raynaud, D., Jouzel, J., Clausen, H.B., Hammer, C.U., Johnsen, S.J., 1998. Asynchrony of Antarctica and Greenland climate during the last glacial period. Nature 394, 739–743.

Braconnot, P., Marzin, C., Grégoire, L., Mosquet, E., Martí, O., 2008. Monsoon response to changes in Earth's orbital parameters: comparisons between simulations of the Eemian and of the Holocene. Clim. Past Discuss 4 (2), 459–493.

Brauer, A., Allen, J.R.M., Mingram, J., Dulski, P., Wulf, S., Huntley, B., 2007. Evidence for last interglacial chronology and environmental change from Southern Europe. Proc. Natl. Acad. Sci. Unit. States Am. 104 (2), 450–455.

Brown, E.T., Werne, J.P., Lozano-García, S., Caballero, M., Ortega-Guerrero, B., Cabral-Cano, E., Valero-Garcés, B.L., Schwalb, A., Arciniega-Ceballos, A., 2012. Scientific drilling in the basin of Mexico to evaluate climate history, hydrological resources, and seismic and volcanic hazards. Sci. Drill. 14, 72–75.

Burjachs, F., López-García, J.M., Allué, E., Blain, H., Rivals, F., Bennàsar, M., Expósito, I., 2012. Palaeoecology of Neanderthals during Dansgaard-Oeschger cycles in northeastern Iberia (abric Romaní): from regional to global scale. Quat. Int. 247, 26–37.

Camuera, J., Jiménez-Moreno, G., Ramos-Román, M.J., García-Alix, A., Toney, J.L., Scott Anderson, R., Jiménez-Espejo, F., Kaufman, D., Bright, J., Webster, C., Yanes, Y., Carrión, J.S., Ohkouchi, N., Suga, H., Yamame, M., Yokoyama, Y., Martínez-Ruiz, F., 2018. Orbital-scale environmental and climatic changes recorded in a new ~200,000-year-long multiproxy sedimentary record from Padul, southern Iberian Peninsula. Quat. Sci. Rev. 198, 91–114.

Camuera, J., Jiménez-Moreno, G., Ramos-Román, M.J., García-Alix, A., Toney, J.L., Anderson, R.S., Jiménez-Espejo, F., Bright, J., Webster, C., Yanes, Y., Carrión, J.S., 2019. Vegetation and climate changes during the last two glacial-interglacial cycles in the western Mediterranean: a new long pollen record from Padul (southern Iberian Peninsula). Quat. Sci. Rev. 86–105.

Carrión, J.S., 1992. Late quaternary pollen sequence from Carihuela Cave, southern Spain. Rev. Palaeobot. Palynol. 71, 37–46.

Carrión, J.S., Leroy, S.A., 2010. Iberian floras through time: land of diversity and survival. Rev. Palaeobot. Palynol. 162 (3), 227–542.

Carrión, J.S., Fernández, S., González-Sampériz, P., Gil-Romera, G., Badal, E., Carrión-Marco, Y., López-Merino, L., López-Sáez, J.A., Fierro, E., Burjachs, F., 2010. Expected trends and surprises in the Lateglacial and Holocene vegetation history of the Iberian Peninsula and Balearic Islands. Rev. Palaeobot. Palynol. 162, 458–475.

Carrión, J.S., Fernández, S., González, P., López, L., Peña, L., Burjachs, F., López-

Sáez, J.A., García-Antón, M., Carrión, Y., Uzquiano, P., Postigo, J.M., Barrón, E., Allué, E., Badal, E., Dupré, M., Fierro, E., Munuera, M., Rubiales, J.M., García, I., Jiménez, G., Gil, G., Leroy, S., García, M.S., Montoya, E., Fletcher, W., Yll, E., Vieira, M., Rodríguez, M.O., Anderson, S., Peñalba, C., Gil, M.J., Pérez, A., Albert, R.M., Díez, M.J., Morales, C., Gómez, F., Parra, I., Ruiz, B., Riera, S., Zapata, L., Ejarque, A., Vegas, T., Rull, V., Scott, L., Abel, D., Andrade, A., Manzano, S., Navarro, C., Pérez, S., Moreno, E., Hernández, L., Sánchez, J., Riquelme, J.A., Iglesias, R., Franco, F., Chaín, C., Figueiral, I., Grau, E., Matos, M., Jiménez, F., Valle, M., Rivas, R., Arribas, A., Garrido, G., Muñiz, F., Finlayson, G., Finlayson, C., Ruiz, M., Pérez, G., Miras, Y., 2013. Paleoflora y Paleovegetación de la Península Ibérica e Islas Baleares: Plioceno-Cuaternario. Ministerio de Economía y Competitividad, Madrid.

Chapman, M.R., Shackleton, N.J., 1999. Global ice-volume fluctuations, North Atlantic ice-rafting events, and deep-ocean circulation changes between 130 and 70 ka. Geology 27, 795–817.

Chen, C., Litt, T., 2018. Dead Sea pollen provides new insights into the paleoenvironment of the southern Levant during MIS 6-5. Quat. Sci. Rev. 188, 15–27.

Connolly, R., Jambrina-Enríquez, M., Herrera-Herrera, A.V., Vidal-Matutano, P., Fagoaga, A., Marquina-Blasco, R., Marín-Monfort, M.D., Ruiz-Sánchez, F.J., Laplana, C., Bailon, S., Pérez, L., Leierer, L., Hernández, C.M., Galván, B., Pérez, L., 2019. A multiproxy record of palaeoenvironmental conditions at the Middle Palaeolithic site of Abric del Pastor (Eastern Iberia). Quat. Sci. Rev. 225, 106023.

Cuffey, K.M., Marshall, S.J., 2000. Substantial contribution to sea-level rise during the last interglacial from the Greenland ice sheet. Nature 404, 591–594.

Dabrio, C.J., Zazo, C., Cabero, A., Goy, J.L., Bardají, T., Hillaire-Marcel, C., González-Delgado, J.A., Lario, J., Silva, P., Borja, F., García-Blázquez, A.M., 2011. Millennial/submillennial scale sea-level fluctuations in western Mediterranean during the second highstand of MIS 5e. Quat. Sci. Rev. 30, 335–346.

Dansgaard, W., Johnsen, S.J., Clausen, H.B., Dahl-Jensen, D., Gundestrup, N.S., Hammer, C.U., Hvidberg, C.S., Steffensen, J.P., Sveinjörnsdottir, A.E., Jouzel, J., Bond, G., 1993. Evidence for general instability of past climate from a 250-kyr ice core record. Nature 364, 218–220.

de Beaulieu, J.L., Reille, M., 1989. The transition from temperate phases to stadials in the long Upper Pleistocene sequence from Les Echets (France). Palaeogeogr. Palaeoclimatol. Palaeoecol. 72, 147–159.

de Beaulieu, J.L., Reille, M., 1992a. Long Pleistocene pollen sequences from the Velay plateau (Massif central, France). Veg. Hist. Archaeobotany 1, 233–242.

de Beaulieu, J.L., Reille, M., 1992b. The last climatic cycle at La Grande Pile (Vosges, France), a new pollen profile. Quat. Sci. Rev. 11 (4), 431–438.

Drescher-Schneider, R., 2000. The Riss-Wurm interglacial from west to east in the Alps: an overview of the vegetational succession and climatic development. Geol. Mijnbouw 79, 233–240.

Drysdale, R.N., Hellstrom, J., Zanchetta, G., Fallick, A.E., Sánchez Goñi, M.F., Couchoud, I., McDonald, J., Maas, R., Lohmann, G., Isola, I., 2009. Evidence for obliquity forcing of glacial termination II. Science 325, 1527–1531.

Fernández, S., Fuentes, N., Carrión, J.S., González-Sampériz, P., Montoya, E., Gil, G., Vega-Toscano, G., Riquelme, J.A., 2007. The Holocene and Upper Pleistocene pollen sequence of Carihuela cave, southern Spain. Geobios 40, 75–90.

Fletcher, W.J., Sánchez Goñi, M.F., 2008. Orbital- and sub-orbital-scale climate impacts on vegetation of the western Mediterranean basin over the last 48,000 yr. Quat. Res. 70 (3), 451–464.

Fletcher, W., Sánchez Goñi, M.F., Allen, J.M.R., Cheddadi, R., Combourieu-Nebout, N., Huntley, B., Lawson, I., Londeix, L., Magri, D., Margari, V., Müller, U.C., Naughton, F., Novenko, E., Roucoux, K., Tzedakis, P.C., 2010. Millennial-scale variability during the last glacial in vegetation records from Europe. Quat. Sci. Rev. 29, 2839–2864.

Follieri, M., Magri, D., Sadori, L., 1988. A 250,000-year pollen record from Valle di Castiglione (Roma). Pollen Spores 30, 329–356.

Foster, G., Royer, D.L., Lunt, D.J., 2017. Future climate forcing potentially without precedent in the last 420 million years. Nat. Commun. 8, 14845.

Fritz, S.C., Baker, P.A., Seltzer, G.O., Ballantyne, A., Tapia, P., Cheng, H., Edwards, R.L., 2007. Quaternary glaciation and hydrologic variation in the South American tropics as reconstructed from the Lake Titicaca drilling project. Quat. Res. 68, 410–420.

Galán, L., Vegas, J., Gallardo-Millán, J.L., Ruiz-Zapata, M.B., Gil-García, M.J., Ortiz, J.E., Moreno, L., García-Cortés, A., Torres, T., 2012. Identificación de episodios climáticos fríos mediante el registro de susceptibilidad magnética en la secuencia lacustre del maar del Fuentillejo (Ciudad Real). Geotemas 13 (1–4), 232.

Gallup, C.D., Edwards, R.L., Johnson, R.G., 1994. The timing of high sea levels over the past 200,000 years. Science 263, 796–800.

García, D., Zamora, R., Hódar, J.A., Gómez, J.M., 1999. Age structure of Juniperus communis L. In the Iberian Peninsula: conservation of remnant populations in Mediterranean mountains. Biol. Conserv. 87, 215–220.

García-Moreiras, I., Delgado, C., Martínez-Carreno, N., García-Gil, S., Muñoz-Sobrino, C., 2019. Climate and vegetation changes in coastal ecosystems during the Middle Pleniglacial and the early Holocene: two multi-proxy, high-resolution records from Ría de Vigo (NW Iberia). Global Planet. Change 176, 100–122.

García-Ruiz, J.M., Valero-Garcés, B.L., Martí-Bono, C., González-Sampériz, P., 2003. Asynchroneity of maximum glacier advances in the central Spanish Pyrenees. J. Quat. Sci. 18, 61–72.

Gasse, F., Vidal, L., Van Campo, E., Demory, F., Develle, A.-L., Tachikawa, K., Elias, A., Bard, E., Garcia, M., Sonzogni, C., Thouveny, N., 2015. Hydroclimatic changes in northern Levant over the past 400,000 years. Quat. Sci. Rev. 111, 1–8.

Gil-García, M.J., Ruiz-Zapata, M.B., Rubio-Jara, S., Panera, J., Pérez-González, A., 2019.

Landscape evolution during the Middle and late Pleistocene in the Madrid basin (Spain): vegetation dynamics and human activity in the Jarama-Manzanares rivers (Madrid) during the Pleistocene. Quat. Int. 520, 39–48.

Gómez-Orellana, L., Ramil-Rego, P., Muñoz Sobrino, C., 2007. The Würm in NW Iberia, a pollen record from area Longa (Galicia). Quat. Res. 67, 438–452.

González-Sampériz, P., Valero-Garcés, B.L., Moreno, A., Jalut, G., García-Ruiz, J.M., Martí-Bono, C., Delgado-Huertas, A., Navas, A., Otto, T., Dedoubat, J.J., 2006. Climate variability in the Spanish Pyrenees during the last 30,000 yr revealed by the El Portalet sequence. Quat. Res. 66, 38–52.

González-Sampériz, P., Leroy, S.A.G., Carrión, J.S., Fernández, S., García-Antón, M., Gil-García, M.J., Uzquiano, P., Valero-Garcés, B., Figueiral, I., 2010. Steppes, savannahs, forests and phytodiversity reservoirs during the Pleistocene in the Iberian Peninsula. Rev. Palaeobot. Palynol. 162, 427–457.

González-Sampériz, P., García-Prieto, E., Aranbarri, J., Valero-Garcés, B.L., Moreno, A., Gil-Romera, G., Sevilla-Callejo, M., Santos, L., Morellón, M., Mata, P., Andrade, A., Carrión, J.S., 2013. Reconstrucción paleoambiental del último ciclo glacial en la Iberia continental: la secuencia del Cañizar de Villarquemado (Teruel). Cuadernos de Investigación Geográfica 39, 49–76.

Govin, A., Capron, E., Tzedakis, P.C., Verheyden, S., Ghaleb, B., Hillaire-Marcel, C., St-Onge, G., Stoner, J.S., Bassinot, F., Bazin, L., Blunier, T., Combourieu-Nebout, N., El Ouahabi, A., Genty, D., Gersonde, R., Jimenez-Amat, P., Landais, A., Martrat, B., Masson-Delmotte, V., Parrenin, F., Seidenkrantz, M.-S., Veres, D., Waelbroeck, C., Zahn, R., 2015. Sequence of events from the onset to the demise of the last interglacial: evaluating strengths and limitations of chronologies used in climatic archives. Quat. Sci. Rev. 129, 1–36.

Gracia, F.J., Gutiérrez, F., Gutiérrez, M., 2003. The Jiloca karst polje-tectonic graben (Iberian Range, NE Spain). Geomorphology 52, 215–231.

Granda, E., Rossatto, D.R., Camarero, J.J., Voltas, J., Valladares, F., 2014. Growth and carbon isotopes of Mediterranean trees reveal contrasting responses to increased carbon dioxide and drought. Oecologia 174, 307–317.

Guan, Q., Pan, B., Gao, H., Li, B., Wang, J., Su, H., 2007. Instability characteristics of the East Asian Monsoon recorded by high-resolution loess sections from the last interglacial (MIS5). Sci. China Series D 7, 1067–1075.

Guiot, J., Cheddadi, R., 2004. Variabilité des écosystèmes terrestres et du climat sur un cycle glaciaire-interglaciaire. Compt. Rendus Geosci. 336, 667–675.

Gutiérrez, F., Gutiérrez-Elorza, M., Gracia, F.J., McCalpin, J.P., Lucha, P., Guerrero, J., 2008. Plio-Quaternary extensional seismotectonics and dreinage natural development in the central sector of the Iberian Chain (NE Spain). Geomorphology 102, 21–42.

Gutiérrez, F., Gracia, F.J., Gutiérrez, M., Lucha, P., Guerrero, J., Carbonel, D., Galve, J.P., 2012. A review on Quaternary tectonic and nontectonic faults in the central sector of the Iberian Chain, NE Spain. J. Iber. Geol. 38 (1), 145–160.

Harting, P., 1875. Le systeme eemien. Archives Neerl. Sci. Exactes Nat. Soc. Holl. des Sci. (Harlem) 10, 443–454.

Heiri, O., Brooks, S.J., Renssen, H., Bedford, Q.A., Hazekamp, M., Ilyashuk, B., Jeffers, E.S., Lang, B., Kirilova, E., Kuiper, S., Millet, L., Samartin, S., Toth, M., Verbruggen, F., Watson, J.E., van Arsch, N., Lammertsma, E., Amon, L., Birks, H.H., Birks, H.J.B., Mortensen, M.F., Hoek, W.Z., Magyari, E., Sobrino, C.M., Seppä, H., Tinner, W., Tonkov, S., Veski, S., Lotter, A.F., 2014. Validation of climate model-inferred regional temperature change for late-glacial Europe. Nat. Commun. 5, 4914.

Helmens, K.F., 2014. The Last Interglacial-Glacial cycle (MIS 5-2) re-examined based on long proxy records from central and northern Europe. Quat. Sci. Rev. 86, 115–143.

Helmens, K.F., Salonen, J.S., Plikk, A., Engels, S., Väliranta, M., Kylander, M., Brendryen, J., Renssen, H., 2015. Major cooling intersecting peak Eemian Interglacial warmth in northern Europe. Quat. Sci. Rev. 122, 293–299.

Höbig, N., Weber, M.E., Kehl, M., Weniger, G.C., Julià, R., Melles, M., Fülöp, R.K., Vogel, H., Reicherter, K., 2012. Lake Banyoles (northeastern Spain): a Last Glacial to Holocene multiproxy study with regard to environmental variability and human occupation. Quat. Int. 274, 205–218.

Hughes, P.D., Woodward, J.C., 2008. Timing of glaciation in the Mediterranean mountains during the last cold stage. J. Quat. Sci. 23, 575–588.

Hughes, P.D., Gibbard, P.L., Ehlers, J., 2013. Timing of glaciation during the last glacial cycle: evaluating the concept of a global 'Last Glacial Maximum' (LGM). Earth Sci. Rev. 125, 171–198.

IPCC, 2014. Climate Change 2014: Mitigation of Climate Change. Cambridge University Press, Cambridge, UK.

Juggins, S., 2012. Rioja: Analysis of Quaternary Science Data, Version 0.7-3. https://cran.r-project.org/web/packages/rioja/index.html.

Kageyama, M., Merkel, U., Otto-Bliesner, B., Prange, M., Abe-Ouchi, A., Lohmann, G., Ohgaito, R., Roche, D.M., Singarayer, J., Swingedouw, D., Zhang, X., 2013. Climatic impacts of fresh water hosing under Last Glacial Maximum conditions: a multi-model study. Clim. Past 9, 935–953.

Klotz, S., Guiot, J., Mosbrugger, V., 2003. Continental European Eemian and early Würmian climate evolution: comparing signals using different quantitative reconstruction approaches based on pollen. Global Planet. Change 36 (4), 277–294.

Kukla, G.J., Bender, M.L., de Beaulieu, J.L., Bond, G., Broecker, W.S., Cleveringa, P., Gavin, J.E., Herbert, T.D., Imbrie, J., Jouzel, J., Keigwin, L.D., Knudsen, K.-L., McManus, J., Merkt, J., Muhs, D.R., Muller, H., Poore, R.Z., Porter, S.C., 2002. Last interglacial climates. Quat. Res. 58 (1), 2–13.

Lacey, J.H., Leng, M.J., H€obig, N., Reed, J.M., Valero-Garcés, B., Reicherter, K., 2016. Western Mediterranean climate and environment since marine isotope stage 3: a 50,000-year record from Lake Banyoles, Spain. J. Paleolimnol. 55, 113–128.

Laskar, J., Robutel, P., Joutel, F., Gastineau, M., Correia, A.C.M., Levrard, B., 2004. A long-term numerical solution for the insolation quantities of the Earth. Astron. Astrophys. 428, 261–285.

Lewis, C.J., McDonald, E.V., Sancho, C., Peña, J.L., Rhodes, E.J., 2009. Climatic implications of correlated Upper Pleistocene glacial and fluvial deposits on the Cinca and Gállego Rivers (NE Spain) based on OSL dating and soil stratigraphy. Global Planet. Change 67, 141–152.

Lisiecki, L.E., Raymo, M.E., 2005. A Pliocene-Pleistocene stack of 57 globally distributed benthic d18O records. Paleoceanography 20 (1), 1–17.

Litt, T., Krastel, S., Sturm, M., Kipfer, R., Örcen, S., Heumann, G., Franz, S.O., Ülgen, U.B., Niessen, F., 2009. PALEOVAN', international continental scientific drilling program (ICDP): site survey results and perspectives. Quat. Sci. Rev. 28, 1555–1567.

Lotter, A., 2003. Multi-proxy climatic reconstructions. In: Mackay, A., Battarbee, R.W., Birks, H.J.B., Oldfield, F. (Eds.), Global Change in the Holocene, pp. 373–383.

Ludwig, P., Shao, Y., Kehl, M., Wenigerd, G.C., 2018. The Last Glacial Maximum and Heinrich event I on the Iberian Peninsula: a regional climate modelling study for understanding human settlement patterns. Global Planet. Change 170, 34–47.

Magri, D., Tzedakis, P.C., 2000. Orbital signatures and long-term vegetation patterns in the Mediterranean. Quat. Int. 73, 69–78.

Martínez-Ferri, E., Manrique, E., Valladares, F., Balaguer, L., 2004. Winter photoinhibition in the field involves different processes in four co- occurring Mediterranean tree species. Tree Physiol. 24, 981–990.

Martrat, B., Grimalt, J.O., Lopez-Martinez, C., Cacho, I., Sierro, F.J., Flores, J.A., Zahn, R., Canals, M., Curtis, J.A., Hodell, D.A., 2004. Abrupt temperature changes in the western Mediterranean over the past 250,000 years. Science 306, 1762–1765.

Martrat, B., Jimenez-Amat, P., Zahn, R., Grimalt, J.O., 2014. Similarities and dissimilarities between the last two deglaciations and interglaciations in the North Atlantic region. Quat. Sci. Rev. 99, 122–134.

Médail, F., Diadema, K., 2009. Glacial refugia influence plant diversity patterns in the Mediterranean Basin. J. Biogeogr. 36, 1333–1345.

Melles, M., Brigham-Grette, J., Minyuk, P.S., Nowaczyk, N.R., Wennrich, V., DeConto, R.M., Anderson, P.M., Andreev, A.A., Coletti, A., Cook, T.L., HaltiaHovi, E., Kukkonen, M., Lozhkin, A.V., Rosen, P., Tarasov, P., Vogel, H., Wagner, B., 2012. 2.8 million years of arctic climate change from Lake El'gygytgyn, NE Russia. Science 337 (6092), 315–320.

Milner, A.M., Müller, U.C., Roucoux, K.H., Collier, R.E.L., Pross, J., Kalaitzidis, S., Christanis, A., Tzedakis, P.C., 2013. Environmental variability during the Last Interglacial: a new high-resolution pollen record from Tenaghi Philippon, Greece. J. Quat. Sci. 28, 113–117.

Monastersky, R., 2015. Anthropocene: the human age. Nature 519, 144–147.

Mommersteeg, H.J.P.M., Loutre, M.F., Young, R., Wijmstra, T.A., Hooghiemstra, H., 1995. Orbital forced frequencies in the 975,000 year pollen record from Tenagi Philippon (Greece). Clim. Dynam. 11, 4–24.

Moore, P.D., Webb, J.A., Collison, M.E., 1991. Pollen Analysis. Blackwell Scientific, Oxford, p. 216.

Morellón, M., Valero-Garcés, B., Vegas-Vilarrúbia, T., González-Sampériz, P., Romero, Ó., Delgado-Huertas, A., Mata, P., Moreno, A., Rico, M., Corella, J.P., 2009. Lateglacial and Holocene palaeohydrology in the western Mediterranean region: the lake Estanya record (NE Spain). Quat. Sci. Rev. 28, 2582–2599.

Morellón, M., Aranbarri, J., Moreno, A., González-Sampériz, P., Valero-Garcés, B.L., 2018. Early Holocene humidity patterns in the Iberian Peninsula reconstructed from lake, pollen and speleothem records. Quat. Sci. Rev. 181, 1–18.

Moreno, A., Valero-Gárcés, B.L., Jiménez-Sánchez, M., Domínguez, M.J., Mata, P., Navas, A., González-Sampériz, P., Stoll, H., Farias, P., Morellón, M., Corella, P., Rico, M., 2010. The last deglaciation in the Picos de Europa National Park (Cantabrian mountains, northern Spain). J. Quat. Sci. 25, 1076–1091.

Moreno, A., González-Sampériz, P., Morellón, M., Valero-Garcés, B.L., Fletcher, W.J., 2012. Northern Iberian abrupt climate change dynamics during the last glacial cycle: a view from lacustrine sediments. Quat. Sci. Rev. 36, 139–153.

Müller, U.C., 2000. A Late-Pleistocene pollen sequence from the Jammertal, southwestern Germany with particular reference to location and altitude as factors determining Eemian forest composition. Veg. Hist. Archaeobotany 9, 125–131.

Müller, U.C., Pross, J., Bibus, E., 2003. Vegetation response to rapid climate change in Central Europe during the past 140,000 yr based on evidence from the Füramoos pollen record. Quat. Res. 59, 235–245.

Muñoz-Sobrino, C., Ramil-Rego, P., Gómez-Orellana, L., 2004. Vegetation of the Lago de Sanabria area (NW Iberia) since the end of the Pleistocene: a palaeoecological reconstruction on the basis of two new pollen sequences. Veg. Hist. Archaeobotany 13, 1–22.

Nikolova, I., Yin, Q., Berger, A., Singh, U.K., Karami, M.P., 2013. The last interglacial (Eemian) climate simulated by LOVECLIM and CCSM3. Clim. Past 9, 1789–1806.

Ninyerola, M., Pons, X., Roure, J.M., 2005. Atlas Climático Digital de la Península Ibérica. Metodología y aplicaciones en bioclimatología y geobotánica. Universidad Autónoma de Barcelona, Bellaterra, Spain.

Okuda, M., Yasuda, Y., Setoguchi, T., 2001. Middle to late Pleistocene vegetation history and climatic changes at lake Kopais, Southeast Greece. Boreas 30, 73–82.

Ortiz, J.E., Moreno, L., Torres, T., Vegas, J., Ruiz-Zapata, B., García-Cortés, A., Galán, L., Pérez-González, A., 2013. A 220 ka palaeoenvironmental reconstruction of the Fuentillejo maar lake record (Central Spain) using biomarker analysis. Org. Geochem. 55, 85–97.

Peñuelas, J., Terradas, J., Lloret, F., 2011. Solving the conundrum of plant species coexistence: water in space and time matters most. New Phytol. 189, 5–8.

Pérez-Mejías, C., Moreno, A., Sancho, C., Martín-García, R., Spötl, C., Cacho, I., Cheng, H., Edwards, R.L., 2019. Orbital-to-millennial scale climate variability during marine isotope stages 5 to 3 in Northeast Iberia. Quat. Sci. Rev. 224, 105946.

Pérez-Obiol, R., Julià, R., 1994. Climatic change on the Iberian Peninsula recorded in a 30,000-yr pollen record from lake Banyoles. Quat. Res. 41, 91–98.

Pickarski, N., Kwiecien, O., Djamali, M., Litt, T., 2015. Vegetation and environmental changes during the last interglacial in eastern Anatolia (Turkey): a new high-resolution pollen record from Lake Van. Palaeogeogr. Palaeoclimatol. Palaeoecol. 435, 145–158.

Pini, R., Ravazzi, C., Donegana, M., 2009. Pollen stratigraphy, vegetation and climate history of the last 215 ka in the Azzano Decimo core (plain of Friuli, northeastern Italy). Quat. Sci. Rev. 28, 1268–1290.

Pons, A., Reille, M., 1988. The Holocene-and upper Pleistocene pollen record from Padul (Granada, Spain): a new study. Palaeogeogr. Palaeoclimatol. Palaeoecol. 66, 243–249.

Pons, A., Guiot, J., De Beaulieu, J.L., Reille, M., 1992. Recent contributions to the climatology of the last glacial-interglacial cycle based on French pollen sequences. Quat. Sci. Rev. 11, 439–448.

Rasmussen, S.O., Bigler, M., Blockley, S.P., Blunier, T., Buchardt, S.L., Clausen, H.B., Cvijanovic, I., Dahl-Jensen, D., Johnsen, S.J., Fischer, H., Gkinis, V., Guillevic, M., Hoek, W.Z., Lowe, J.J., Pedro, J.B., Popp, T., Seierstad, I.K., Steffensen, J.P., Svensson, A.M., Vallelonga, P., Vinther, B.M., Walker, M.J.C., Wheatley, J.J., Winstrup, M., 2014. A stratigraphic framework for abrupt climatic changes during the Last Glacial period based on three synchronized Greenland ice-core records: refining and extending the INTIMATE event stratigraphy. Quat. Sci. Rev. 106, 14–28.

Reille, M., 1992. Pollen et spores d'Europe et d'Afrique du Nord. Laboratoire de botanique historique et de palynologie, Marseille, p. 520.

Roberts, N., 1998. The Holocene: an Environmental History, third ed. Wiley-Blackwell, p. 376.

Rodbell, D.T., Abbott, M.B., 2012. Workshop on drilling of Lake Junin, Peru: potential for development of a continuous tropical climate record. Sci. Drill. 13, 58–60.

Rohling, E.J., Grant, K., Hemleben, Ch., Siddall, M., Hoogakker, B.A.A., Bolshaw, M., Kucera, M., 2008. High rates of sea-level rise during the last interglacial period. Nat. Geosci. 1, 38–42.

Rubiales, J.M., García-Amorena, I., Hernández, L., Génova, M., Martínez, F., Manzaneque, F.G., Morla, C., 2010. Late quaternary dynamics of pinewoods in the Iberian mountains. Rev. Palaeobot. Palynol. 162, 476–491.

Rubio, J.C., 2004. Contexto hidrogeológico e histórico de los humedales del Cañizar. Consejo de la Protección de la Naturaleza de Aragón, Serie de Investigación, Zaragoza.

Rubio, J.C., Simon, J.L., 2007. Tectonic subsidence v, erosional lowering in a controversial intramontane depression: the Jiloca basin (Iberian Chain, Spain). Geol. Mag. 144, 127–141.

Ruiz-Zapata, B., Vegas, J., Gil-García, M.J., Gallardo-Millán, J.L., Ortiz, J.E., Moreno, L., Galán, L., García-Cortés, A., Torres, T., 2012. Registro polínico durante el Saaliense-Eemiense en la secuencia lacustre del maar del Fuentillejo (Ciudad Real). Geotemas 13, 245.

Sadori, L., Koutsodendris, A., Masi, A., Bertini, A., Combourieu-Nebout, N., Francke, A., Kouli, K., Joannin, S., Mercuri, A.M., Peyron, O., Torri, P., Wagner, B., Zanchetta, G., Sinopoli, G., Donders, T.H., 2016. Pollen-based paleoenvironmental and paleoclimatic change at Lake Ohrid (SE Europe) during the past 500 ka. Biogeosciences 13, 1423–1437.

Sainz Ollero, H., Van Staalduinen, M., 2012. Iberian steppes. In: Werger, M.J.A., van Staalduinen, M.A. (Eds.), Eurasian Steppes. Ecological Problems and Livelihoods in a Changing World. Springer, Dordrecht, Netherland, pp. 273–288.

Sánchez Goñi, M.F., 2005. Introduction to climate and vegetation in Europe during MIS5. Dev. Quat. Sci. 7, 197–205.

Sánchez Goñi, M.F., 2006. Interactions végétation-climat au cours des derniers 425.000 ans en Europe occidentale. Le message du pollen des archives marines. Quaternaire 17–1, 3–25.

Sanchez Goñi, M.F., Harrison, S.P., 2010. Millennial-scale climate variability and vegetation changes during the Last Glacial: concepts and terminology. Quat. Sci. Rev. 29 (21–22), 2823–2827.

Sánchez Goñi, M.F., Eynaud, F., Turon, J.L., Shackleton, N.J., 1999. High resolution palynological record off the Iberian margin: direct land-sea correlation for the Last Interglacial complex. Earth Planet Sci. Lett. 171, 123–137.

Sánchez Goñi, M.F., Turon, J.L., Eynaud, F., Shackleton, N.J., Cayre, O., 2000. Direct land−sea correlation of the Eemian and its comparison with the Holocene: a high resolution palynological record off the Iberian margin. Geol. Mijnbouw 79, 345–354.

Sánchez Goñi, M.F., Loutre, M.F., Crucifix, M., Peyron, O., Santos, L., Duprat, J., Malaizé, B., Turon, J.L., Peypouquet, J.P., 2005. Increasing vegetation and climate gradient in Western Europe over the Last Glacial Inception (122−110 ka): data-model comparison. Earth Planet Sci. Lett. 231 (1−2), 111−130.

Sanchez Goñi, M.F., Bakker, P., Desprat, S., Carlson, A.E., Van Meerbeeck, C.J., Peyron, O., Naughton, F., Fletcher, W.J., Eynaud, F., Rossignol, L., Renssen, H., 2012. European climate optimum and enhanced Greenland melt during the Last Interglacial. Geology 40 (7), 627−630.

Sánchez de Dios, R., Velázquez, J.C., Sainz Ollero, H., 2019. Classification and mapping of Spanish Mediterranean mixed forests. iFor. Biogeosci. For. 12 (5), 480.

Sancho, C., Arenas, C., Pardo, G., Peña-Monné, J.L., Rhodes, E.J., Bartolomé, M.,

19

García-Ruiz, J.M., Martí-Bono, C., 2018. Glaciolacustrine deposits formed in an ice-dammed tributary valley in the south-central Pyrenees: new evidence for late Pleistocene climate. Sediment. Geol. 366, 47–66.

Satkunas, J., Grigiene, A., Velichkevich, F., Robertsson, A., Sandgren, P., 2003. Upper Pleistocene stratigraphy at the Medininkai site, eastern Lithuania: a continuous record of the EemianWeichselian sequence. Boreas 32, 627–641.

Shackleton, N.J., Hall, H.A., Vincent, E., 2000. Phase relationships between millennial-scale events 64,000-24,000 760 years ago. Paleoceanography 15, 565–569.

Shackleton, N.J., Sanchez-Goñi, M.F., Paillerc, D., Lancelot, Y., 2003. Marine Isotope Substage 5e and the Eemian Interglacial. Global Planet. Change 36, 151–155.

Siddall, M., Rohling, E., Almogi-Labin, A., 2003. Sea-level fluctuations during the last glacial cycle. Nature 423, 19–24.

Sier, M.J., Roebroeks, W., Bakels, C.C., Dekkers, M.J., Brühl, E., De Loecker, D., Gaudzinski-Windheuser, S., Hesse, N., Jagich, A., Kindler, L., Kuijper, W.J., Laurat, T., Mücher, H.J., Penkman, K.E.H., Richter, D., van Hinsbergen, D.J.J., 2011. Direct terrestrial–marine correlation demonstrates surprisingly late onset of the last interglacial in central Europe. Quat. Res. 75, 213–218.

Sinopoli, G., Masi, A., Regattieri, E., Wagner, B., Francke, A., Peyron, O., Sadori, L., 2018. Palynology of the last interglacial complex at Lake Ohrid: palae-oenvironmental and palaeoclimatic inferences. Quat. Sci. Rev. 180, 177–192.

Sirocko, F., Claussen, M., Sánchez Goñi, F.M., Litt, T., 2007. The climate of past interglacials. In: Developments in Quaternary Science, vol. 7. Elsevier, Amsterdam, p. 622.

Stockmar, J., 1971. Tablets spores used in absolute pollen analysis. Pollen Spores 13, 615–621.

Stoll, H.M., Moreno, A., Méndez-Vicente, A., González-Lemos, S., Jiménez-Sánchez, M., Domínguez-Cuesta, M.J., Edwards, L.R., Cheng, H., Wang, X., 2013. Paleoclimate and growth rates of speleothems in the northwestern Iberian Peninsula over the last two glacial cycles. Quat. Res. 80, 284–290.

Terrab, A., Schönswetter, P., Talavera, S., Vela, E., Stuessy, T.F., 2008. Range-wide phylogeography of Juniperus thurifera L, a presumptive keystone species of western Mediterranean vegetation during cold stages of the Pleistocene. Mol. Phylogenet. Evol. 48, 94–102.

Teixeira, H., Rodríguez-Echeverría, S., Nabais, C., 2014. Genetic diversity and differentiation of Juniperus thurifera in Spain and Morocco as determined by SSR. PloS One 9 (2), e88996.

Torner, J., Cacho, I., Moreno, A., Sierro, F.J., Martrat, B., Rodríguez-Lázaro, J., Frigola, J., Arnau, P., Belmonte, A., Hellstrom, J., Cheng, H., Edwards, R.L., Stoll, H., 2019. Ocean-atmosphere interconnections from the last interglacial to the early glacial: an integration of marine and cave records in the Iberian region. Quat. Sci. Rev. 226, 106037.

Tzedakis, P.C., 1994. Vegetation change through glacial-interglacial cycles: a long pollen sequence perspective. Phil. Trans. Roy. Soc. Lond. B Biol. Sci. 345, 403–432.

Tzedakis, P.C., 2005. Towards an understanding of the response of southern European vegetation to orbital and suborbital climate variability. Quat. Sci. Rev. 24, 1585–1599.

Tzedakis, P.C., 2007. Seven ambiguities in the Mediterranean palaeoenvironmental narrative. Quat. Sci. Rev. 26, 2042–2066.

Tzedakis, P.C., Lawson, I.T., Frogley, M.R., Hewitt, G.M., Preece, R.C., 2002. Buffered tree population changes in a quaternary refugium: evolutionary implications. Science 297, 2044–2047.

Tzedakis, P.C., Frogley, M.R., Heaton, T.H.E., 2003. Last Interglacial conditions in southern Europe: evidence from Ioannina, northwest Greece. Global Planet. Change 36, 157–170.

Tzedakis, P.C., Hooghiemstra, H., Pälike, H., 2006. The last 1.35 million years at Tenaghi Philippon: revised chronostratigraphy and long-term vegetation trends. Quat. Sci. Rev. 25 (23–24), 3416–3430.

Tzedakis, P.C., Drysdale, R.N., Margari, V., Skiner, L., Menviel, L., Rhodes, R.H., Taschetto, A.S., Hodell, D.A., Crowhurst, S.J., Hellstrom, J.C., Fallick, A.E., Grimalt, J.O., McManus, J.F., Martrat, B., Mokeddem, Z., Parrenin, F., Regattieri, E., Roe, K., Zanchetta, G., 2018. Enhanced climate instability in the north Atlantic and southern europe during the last interglacial. Nat. Commun. 9, 4235.

Valero-Garcés, B.L., González-Sampériz, P., Romera, G.G., Benito, B.M., Moreno, A., Oliva-Urcia, B., Aranbarri, J., García-prieto, E., Frugone, M., Morellón, M., Arnold, L.J., Demuro, M., Hardiman, M., Blockley, S.P.E., Lane, C.S., 2019. A multi-dating approach to age-modelling long continental records: the 135 ka El Cañizar de Villarquemado sequence (NE Spain). Quat. Geochronol. 54, 101006.

Vegas, J., Ruiz-Zapata, B., Ortiz, J.E., Galán, L., Torres, T., García-Cortés, Á., Gil-García, M.J., Pérez-González, A., Gallardo-Millán, J.L., 2010. Identification of arid phases during the last 50 cal. ka BP from the Fuentillejo maar-lacustrine record (Campo de Calatrava Volcanic Field, Spain). J. Quat. Sci. 25, 1051–1062.

Vidal-Matutano, P., Hernández, C.M., Galván Santos, B., Mallol, C., 2015. Neanderthal firewood management: evidence from Stratigraphic Unit IV of Abric del Pastor (Eastern Iberia). Quat. Sci. Rev. 21 (111), 81–93.

Waelbroeck, C., Labeyrie, L., Michela, E., Duplessy, J.C., McManus, J.F., Lambeck, K., Balbon, E., Labracherie, M., 2002. Sea-level and deep water temperature changes derived from benthic foraminifera isotopic records. Quat. Sci. Rev. 21, 295–305.

Waters, C.N., Zalasiewicz, J., Summerhayes, C., Fairchild, I.J., Rose, N.L., Loader, N.J., Shotyk, W., Cearreta, A., Head, M.J., Syvitski, J.P.M., Williams, M., Wagreich, M., Barnosky, A.D., An, Z., Leinfelder, R., Jeandel, C., Gałuszka, A., Ivar do Sul, J.A., Gradstein, F., Steffen, W., McNeill, J.R., Wing, S., Poirier, C., Edgeworth, M., 2018. Global boundary stratotype section and point (GSSP) for the anthropocene series: where and how to look for potential candidates. Earth Sci. Rev. 178, 379–429.

Wijmstra, T.A., 1969. Palynology of the first 30 metres of a 120 m deep section in northern Greece. Acta Bot. Neerl. 18 (4), 511–527.

Willis, K.J., Rudner, E., Sümegi, P., 2000. The full-glacial forests of central and southeastern Europe. Quat. Res. 53, 203–213.

Woillard, G.M., 1978. Grande Pile peat bog: a continuous pollen record for the last 140,000 years. Quat. Res. 9 (1), 1–21.

Wolf, D., Kolb, T., Alcaraz-Castaño, M., Heinrich, S., Baumgart, P., Calvo, R., Sánchez, J., Ryborz, K., Schäfer, I., Bliedtner, M., Zech, R., Zöller, L., Faust, D., 2018. Climate deteriorations and Neanderthal demise in interior Iberia. Sci. Rep. 8, 7048.

Wulf, S., Keller, J., Paterne, M., Mingram, J., Lauterbach, S., Opitz, S., Sottili, G., Giaccio, B., Albert, P., Satow, C., Tomlinson, E., Viccaro, M., Brauer, A., 2012. The 100-133 ka record of Italian explosive volcanism and revised tephrochronology of Lago Grande di Monticchio. Quat. Sci. Rev. 58, 104–123.

Zalasiewicz, J., Waters, C.N., Summerhayes, C.P., Wolfe, A.P., Barnosky, A.D., Cearreta, A., Crutzen, P., Ellis, E., Fairchild, I.J., Gałuszka, A., Haff, P., Hajdas, I., Head, M.J., Ivar do Sul, J.A., Jeandel, C., Leinfelder, R., McNeill, J.R., Neal, C., Odada, E., Oreskes, N., Steffen, W., Syvitski, J., Vidas, D., 2017. The working group on the anthropocene: summary of evidence and interim recommendations. Anthropocene 19, 55–60.

Zolitschka, B., Schäbitz, F., Lücke, A., Clifton, G., Corbella, H., Ercolano, B., Haberzettl, T., Maidana, N., Mayr, C., Ohlendorf, C., Oliva, G., Páez, M., Schleser, G., Soto, J., Tiberi, P., Wille, M., 2006. Crater lakes of the Pali Aike Volcanic field as key sites for paleoclimatic and palaeoecological reconstructions in southern Patagonia, Argentina. J. S. Am. Earth Sci. 21, 294–309.